Acta Protozool. (2015) 54: 241–263
www.ejournals.eu/Acta-Protozoologica
doi:10.4467/16890027AP.15.020.3217

ACTA
PROTOZOOLOGICA

# Ultrastructure and 28S rDNA Phylogeny of Two Gregarines: *Cephaloidophora* cf. *communis* and *Heliospora* cf. *longissima* with Remarks on Gregarine Morphology and Phylogenetic Analysis

**Timur G. Simdyanov[1], Andrei Y. Diakin[2], Vladimir V. Aleoshin[3]**

**[1] Department of Invertebrate Zoology, Faculty of Biology, Lomonosov Moscow State University, Moscow, Russian Federation; [2] Department of Botany and Zoology, Faculty of Science, Masaryk University, Brno, Czech Republic; [3] Belozersky Institute of Physico-Chemical Biology, Lomonosov Moscow State University, Moscow, Russian Federation**

**Abstract.** 18S rRNA gene sequences (SSU rDNA) in gregarines are problematic for phylogenetic analysis, mainly due to artifacts related to long branch attraction (LBA). In this study, we sequenced 18S rRNA (SSU rRNA), 5.8S rRNA, and 28S rRNA (LSU rRNA) genes of two gregarine species from crustacean hosts (gregarine superfamily Cephaloidophoroidea): *Cephaloidophora* cf. *communis* from a marine cirripedian *Balanus balanus* (White Sea), and *Heliospora* cf. *longissima* from the freshwater amphipods, *Eulimnogammarus verrucosus* and *E. vittatus* (Lake Baikal). Phylogenetic analyses of SSU rDNA sequences failed to produce a robust tree topology, for a limited taxon sample (31 operational taxonomic units (OTU), based on 1,604 sites), while LSU (2,869 sites), and concatenated dataset based on SSU, 5.8S, and LSU (4,627 sites) produced more consistent tree topologies for the same taxon sample. Analyses testing for LBA-influence were negative, therefore we suggested that the main reason of the failed topologies in SSU rDNA analyses is insufficient data (insufficient taxon sampling and limited molecular data), rather than LBA. Possible advantages of Bayesian analyses, compared to Maximum Likelihood, and usage of LSU rDNA within the context of apicomplexan phylogenetics were discussed. One of the advantages of LSU is likely its lower rate of evolution in long-branching apicomplexans (e.g., gregarines), relative to other (non-long-branching) apicomplexans, compared to SSU rDNA. Ultrastructure of the epicytic folds was studied. There are 3 to 5 apical arcs (also known as rippled dense structures) and 2 to 5 apical filaments in the tops of the folds. This small number of the apical structures fits into morphological diversity of the epicyte in other Cephaloidophoroidea, but this is not a synapomorphy of the group because this was also detected in several unrelated gregarines. *C.* cf. *communis* was found to contain a septum between the epimerite and the protomerite, which has not been reported in other gregarines. More exact terminology, which takes into account number of body sections and septa, is proposed for morphological descriptions of trophozoites and free mature gamonts of gregarines. In accordance with this, *C.* cf. *communis* gamonts are tricystid and biseptate, whereas *H.* cf. *longissima* gamonts are tricystid and uniseptate, similar to other eugregarines.

**Key words:** Apicomplexa, gregarines, crustacean host, morphology, ultrastructure, LSU rDNA, molecular phylogeny.

Address for correspondence: Timur G. Simdyanov, Dept. of Invertebrate Zoology, Faculty of Biology, Lomonosov Moscow State University, Leninskiye Gory 1-12, Moscow 119234, Russian Federation; tel./fax: +7 495 939 5695; E-mail: tgsimd@gmail.com

## INTRODUCTION

Gregarines are obligate, unicellular apicomplexan parasites that predominantly infect the digestive system and coelomic cavities of a broad range of marine, freshwater, and terrestrial invertebrates. The feeding and growing stages of gregarines (trophozoites) can reach a large size, compared to the majority of unicellular organisms (up to several millimeters; however, about sizes ranging from 200–500 μm are common). Many of these trophozoite stages are also complex at the ultrastructural and superficial level. In general, gregarines are monoxenous (except members of the family Porosporidae), epicellular parasites; their trophozoites have ovoid or elongated shape and are heteropolar: the cell forebody is used to attach to the host cell.

Traditionally, trophozoites have been divided into either non-segmented (monocystid) forms, or into segmented (polycystid) forms that are compartmentalized by constrictions and/or septa; the latter are further divided into dicystid, tricystid, and multisegmented types (Grassé 1953). Since 1971, all these terms have been replaced with "aseptate" and "septate" (Levine 1971), and are widely used among workers in the field (Perkins *et al*. 2000). However, the traditional terminology has been partially restored in the new edition of "Treatise on Zoology" (Desportes and Schrével 2013).

Septate forms (e.g. *Gregarina, Cephaloidophora, Stylocephalus*) belong to the largest gregarine order, the Eugregarinida (or Eugregarinorida) Léger 1900, which also comprises many aseptate representatives (e.g., *Monocystis, Lecudina,* and *Urospora*). The anterior end of the trophozoite in eugregarines, responsible for the attachment to the host cell has a different cytoplasm structure: its cytoplasm is more translucent (hyaline), while the rest of the cell is more opaque, due to the storage carbohydrate (amylopectin) granules (Mercier *et al*. 1973). This part of the cell is called the "mucron" in aseptate forms, or "epimerite" in septate ones (Levine 1971). Epimerites of gregarines vary in size and shape, being large or small, prolonged or lens-like. They can bear hooks or projections, and often appear to be separated from the rest of the body by a septum.

Tricystid septate forms have a body part called the protomerite, behind the epimerite. The protomerite is followed by the deutomerite, which contains the nucleus. The protomerite and deutomerite are separated by a septum. There are several electron microscopy studies that observed the ultrastructure at the anterior end of septate gregarines. These studies demonstrated that the septum is composed primarily of tightly packed, thin fibrils. However, no such septum has been observed between the epimerite and protomerite (Grassé and Théodoridès 1959, Devauchelle 1968a, Desportes 1969, Baudoin and Ormières 1973, Hoshide 1975, Hildebrand 1976, Ormières 1977, Tronchin and Schrével 1977, Valigurová and Koudela 2005, Valigurová 2012). In *Epicavus araeoceri*, separate radial microtubules, which arise from a putative remnant of the conoid situated at the base of the epimerite, form a structure referred to as the "pseudoseptum" (Ormières and Daumal 1970a, b). In multisegmented (or "metamerized") gregarines (e.g., *Metamera and Taeniocystis*), the deutomerite is subdivided by several additional septa. However, no work has been done on the ultrastructure of these septa. The presence of a septum in the protomerite/deutomerite (using only light microscopy) is considered a diagnostic character of suborders Aseptata (Aseptatorina) and Septata (Septatorina) (Levine 1985, Clopton 2000). When the growth period is over, the epimerite of septate gregarines usually disappears (Grassé 1953), or is condensed (Devauchelle 1968a, Valigurová *et al*. 2009, Valigurová 2012), and the gregarine cells acquire a dicystid-like morphology and (commonly) start to move in the intestine lumen. Under Levine's nomenclature (Levine 1971) this stage is called a "gamont".

The overwhelming majority of eugregarines have gliding motility, and a specific surface structure that is composed of numerous (sometimes hundreds) longitudinal pellicular folds known as epicytic folds. Gregarines have a characteristic tegument represented by a trimembrane pellicle, which consists of the plasmalemma with a cell coat, and the inner membrane complex (IMC) formed by two closely adjacent cytomembranes (Vivier 1968, Vivier *et al*. 1970, Schrével *et al*. 1983). There are micropores in the pellicle located between the epicytic folds, or (rarely) on their sides (Desportes 1969, Simdyanov 1995). Micropores are characteristic structures of apicomplexans, visible only by electron microscope. Specifically, these are small pores on the surface of a cell leading into little invaginations of plasma membrane inside the cytoplasm. The invaginations penetrate the IMC through openings collared by electron-dense material. There are electron-dense longitudinal structures within apical parts of the epicytic folds: "apical arcs" (also called "rippled dense structures") and "apical filaments" (also called "12 nm filaments") (Vivier 1968, Schrével *et al*. 1983). The apical filaments adjoin the IMC from the inner part of the cell

at the top of the folds, and the apical arcs are arranged between the plasmalemma and the IMC from the outer side, and often face the apical filaments (an arc is in front of a filament). The number of these arcs and the filaments is usually 5 to 10–12 (Vivier 1968, Desportes *et al*. 1977, Hildebrand 1981, Walker and Lane 1982, Janardanan and Ramachandran 1983, Schrével *et al*. 1983, Simdyanov 1995, 2004, 2009). Eugregarines lacking gliding motility have various aberrant epicyte structures, or sometimes lack the epicytic folds entirely (Miles 1968, Vinckier and Vivier 1968, Vinckier 1969, Porchet-Henneré and Fischer 1973, MacMillan 1973, Marques *et al*. 1978, Landers 2002, Dyakin and Simdyanov 2005, Landers and Leander 2005).

Motility is necessary to find a sexual partner and to form syzygy, a sexual association of gamonts (Grassé 1953, Levine 1971, Desportes and Schrével 2013). This stage is often considered characteristic for gregarines, although, among apicomplexans, it also exists in adeleid coccidians, for instance, in haemogregarines (Perkins *et al*. 2000). Usually, the syzygy is just a mechanical association of two mature gamonts without fusion of their cytoplasms; however, the contact can be more complex in some cases (Devauchelle 1968b, Desportes 1974, Dallai and Vegni Talluri 1988, Frolov 1991). Septate eugregarines have a "caudo-frontal" (head-to-tail) syzygy where the anterior individual is called "primite" and the posterior one "satellite" (Grassé 1953, Levine 1971). There can be more than one satellite: two, three, or more (Grassé 1953). In some gregarine species, syzygy is formed in feeding (trophozoite) and growth stages (early syzygy). In others, they emerge immediately before formation of the gametocyst (late syzygy). The general ultrastructure of the syzygy partners in septate gregarines is largely similar to that of trophozoites in the same species (Devauchelle 1968b, Desportes 1974, Philippe 1983, Dallai and Vegni Talluri 1988).

A recent system of gregarine classification has been developed by Levine throughout the 1970s and 1980s (Levine 1970, 1979, Levine *et al*. 1980, Levine 1984, 1985, 1988a, b) with minor modifications accepted later (Perkins *et al*. 2000, Adl *et al*. 2012). This system relies on morphological characters of trophozoites, gamonts and syzygy, as well as on certain lifecycle traits. For instance, the order Eugregarinida (=Eugregarinorida) is divided into suborders Aseptata (=Aseptatorina) and Septata (=Septatorina). This assumes that the presence of the protomerite/deutomerite septum is a synapomorphy of the monophyletic taxon "septate eugregarines". The suborder Septata includes four superfamilies: Porosporicae (heteroxenous, one family), Gregarinicae (early syzygies), Stenophoricae (late syzygies), and Fusionicae (gamont cytoplasms fuse in syzygy; one family).

Previous work also established other classification schemes. The most common one was the system by Grassé (1953), based on the concept of co-evolution of gregarines and their hosts. Morphological characters were of secondary importance in this system; it included no suborders or superfamilies, and the families were recognized primarily according to the taxonomic position of their hosts. The presence of the septum was not considered a major taxonomic character. For instance, the aseptate gregarine family Lecudinidae (parasites of polychaetes) comprised the genus *Sycia* with a septum, while the family of septate gregarines, Actinocephalidae (parasites of insects), comprised *Schneideria*, which lacks a septum, a typical tricystid, *Actinocephalus*, and the multisegmented *Taeniocystis*. Grassé (1953) proposed that certain aseptate gregarines secondarily lost the septum ("pseudomonocystid" gregarines). This was proposed for *Lankesteria* (now *Ascogregarina*) *culicis*. Overall, this system upheld that the septa are a labile morphologic formation that repeatedly appeared and disappeared in the evolution of gregarines. Grassé's evolutionary hypotheses were put forth before the use of electron microscopy and molecular methods became established in protist studies.

Still, ultrastructural characters are not entirely applicable for taxonomic studies. This is due to the fact that most gregarine species have been described using light microscopy, which is generally insufficient for phylogenetic inferences (Grassé 1953, Levine 1985, Perkins *et al*. 2000). Moreover, electron microscopic studies of gregarines are fragmentary, and subsequently, our knowledge about different taxa contains uneven levels of detail. Therefore, the more recent use of molecular tools will start to 'fill in the gaps' in our knowledge of species-level diversity and evolutionary relationships between distict and closely-related gregarine lineages.

Contemporary use of molecular phylogenetics in gregarines largely relies on the analysis of small subunit (SSU) rDNA sequences (Leander *et al*. 2003a, b,Leander *et al*. 2006, Leander 2007, Rueckert and Leander 2008, 2009, Clopton, 2009, Rueckert *et al*. 2010, Rueckert and Leander 2010, Rueckert *et al*. 2011a, b, Wakeman and Leander 2012, Rueckert *et al*. 2013, Wakeman and Leander 2013). However, these phylogenetic analyses show high divergence rates among of SSU rDNA sequences in many gregarine clades, mak-

ing nodal-support and the overall topology for some parts of tree susceptible to artifacts such as long branch attraction (LBA). Recent SSU rDNA analyses demonstrated a robust clade of gregarines (Cephaloidophoroidea) parasitic in crustaceans. The Cephaloidophoroidea comprises both aseptate and septate trophozoite forms (Rueckert *et al*. 2011b). In phylogenetic trees, this branch is extremely long and occupies an isolated position (i.e., nodal support between this clade and other gregarine clades is unresolved).

Here we present ultrastructural data on two gregarines species: *Cephaloidophora* cf. *communis* Mawrodiadi, 1908 and *Heliospora* cf. *longissima* (von Siebold in Kölliker 1848) Goodrich, 1949, as well as the results from phylogenetic analyses of large subunit (LSU) rDNA and SSU rDNA datasets.

## MATERIALS AND METHODS

### Collection and isolation of organisms

Both gregarine species were isolated from different crustacean hosts in marine and freshwater habitats. *Cephaloidophora* cf. *communis* was isolated from the intestine of *Balanus balanus* Linnaeus, 1758 (Cirripedia) collected from the White Sea (White Sea Biological Station of Moscow State University, Velikaya Salma Straight, Kandalaksha Gulf, 66°33′12″N, 33°06′17″E, Russia) in 2006. *Heliospora* cf. *longissima* was isolated from the intestines of two freshwater amphipods endemic to Lake Baikal, namely, *Eulimnogammarus verrucosus* Gerstfeldt, 1858, and *Eulimnogammarus vittatus* Dybowski, 1874; both species were collected near the Bolshiye Koty village (51°54′12″N, 105°04′30″E), Lake Baikal, Russia in 2005.

The specimens of each species were released into seawater (*C.* cf. *communis*) or saline solution (150 mM NaCl) (*H.* cf. *longissima*) by tearing apart the intestine of the hosts with fine-tipped needles under a stereomicroscope (MBS-1, LOMO, Russia). The gut material was examined under the stereomicroscope and the parasites were isolated using fine glass pipettes, rinsed three times in either filtered seawater or saline solution depending on the hosts' habitat (marine or freshwater), photographed, fixed for electron microscopy, or prepared for DNA extraction.

### Light microscopy

Some micrographs of *C.* cf. *communis* and *H.* cf. *longissima* were produced using light microscopes (Karl Zeiss, Jena and LOMO, USSR) and a Nikon Coolpix 7900 camera. Differential interference contrast (DIC) light micrographs of *C.*cf. *communis* were produced with a Leica DM 2000 light microscope connected to a Leica DFC 420 camera (Leica Microsystems, Germany).

### Transmission electron microscopy

Several specimens of *C.* cf. *communis* (gamonts) and *H.* cf. *longissima* (gamonts and syzygy) from *E. verrucosus* were prepared for transmission electron microscopy (TEM). The specimens were fixed with 2.5% (v/v) glutaraldehyde in 0.05 M cacodylate buffer (pH 7.4) containing 1.28% (w/v) NaCl in an ice bath, in the dark. Fixative was replaced with a fresh portion after 1 hour; total time for fixation was 2 hours. Fixed samples were rinsed three times with the cacodylate buffer, and post-fixed with 2% (w/v) $OsO_4$ in cacodylate buffer (ice bath, 2 hours). After dehydration in a graded ethanol series, the fixed parasites were embedded in Epon resin using a standard procedure. Ultrathin sections obtained using an LKB-III ultramicrotome (LKB, Sweden) were contrasted with 4% (w/v) water solution of uranyl acetate (40 minutes at 37ºC) and 0.04% (w/v) water solution of lead citrate (Reynolds 1963) for 20 minutes at room temperature in the dark. The sections were examined under a JEM-100B or a JEM 1011 electron microscopes (Jeol, Japan).

### DNA isolation, PCR, and sequencing

Individuals of each species were isolated from the dissected host intestines, washed three times in the appropriate medium, and deposited into 1.5 ml microcentrifuge tubes: 93 individuals of *C.* cf. *communis* from *B. balanus*, 20 individuals of *H.* cf. *longissima* from *E. verrucosus*, and 25 trophozoites of *H.* cf. *longissima* from *E. vittatus*. All samples were subjected to alkaline lysis (Floyd *et al*. 2002) with modifications (Petrov *et al*. 2007). The lysates were used directly for PCR.

The rDNA sequences were amplified in a PCR series, following methods and primers for SSU rDNA amplification described earlier (Rueckert *et al*. 2011b). For the rest of the ribosomal operon, a set of overlapping fragments was obtained (Fig. 1). All fragments were amplified with an Encyclo PCR kit (Evrogen, Russia) in a total volume of 25 µl using a DNA Engine Dyad thermocycler (Bio-Rad) using the following protocol: initial denaturation at 95°C for 3 min; 40 cycles of 95°C for 30 sec, 50°C for 30 sec, and 72°C for 1.5 min; and a final extension at 72°C for 10 min. The fragments were amplified using primers d6 (5′– CCGTTCTTAGTTGGTGG –3′) and 28r2 (5′– TACTTGTYBRCTATCG –3′) for fragment I, d71c (5′– gta-

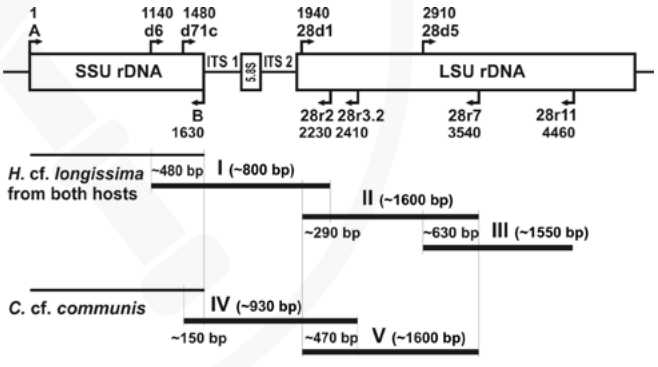


**Fig. 1.** Layout of ribosomal operon fragment amplifications. Upper part, schematic ribosomal operon with approximate positions of the direct and reverse primers used. Lower part, the amplified fragments of ribosomal DNA aligned with the ribosomal operon (above). Numbers indicate the length of the overlapping regions. Roman numerals denote the fragments discussed in this paper. SSU rDNA fragments analyzed previously by Rueckert *et al*. (2011b) have no numerical designations.

cacaccgcccgtcgtttctt –3′) and 28r3.2 (5′– ACTCCTYRGTCCGTGTTTCA –3′) for fragment IV, 28d1 (5′– ACCCGCTGAAYTTAAGCATAT –3′) and 28r7 (5– GCCAATCCTTWTCCCGAAGTTAC –3′) for fragments II and V, and 28d5 (5′– CCGCTAAGGAGTGTGTAACAAC –3′) and 28r11 (5′– GTCTAAACCCAGCTCACGTTCCCT –3′) for fragment III. The LSU rDNA primer sequences are based on van der Auwera *et al*. (1994).

PCR products of the expected sizes (~800 bp for fragment I, ~900 bp for fragment IV, and ~1,600 bp for fragments II, III, and V, also see Fig. 1) were gel isolated using a Cytokine DNA isolation kit (Cytokine, Russia) and sequenced using an ABI PRISM BigDye Terminator v. 3.1 reagent kit on an automatic sequencer Applied Biosystems 3730 DNA Analyzer. DNA sequences were preliminarily identified by BLAST analysis, including the built-in NJ-tree tool. Following this initial BLAST search, fragments were assembled with overlapping counterparts, and with matching parts of SSU rDNA sequences that were obtained earlier from the same gregarine samples (GenBank accession numbers: HQ891113.1 – HQ891115.1). The contigs of the ribosomal operons (SSU rDNA + ITS1 + 5.8S rDNA + ITS2 + LSU rDNA) were constructed for each gregarine sample (GenBank accession numbers: HQ891113.2 – HQ891115.2). Sequence accession numbers from this study are presented in the Table 1.

**Table 1.** List of SSU, 5.8S, and LSU rDNA sequences used in phylogenetic analyses.

| Operational taxonomic unit (OTU) | GenBank accession number | | |
|---|---|---|---|
| | SSU | 5.8S | LSU |
| *Akashiwo sanguinea* | AY831412 | AY831412 | AY831412 |
| *Alexandrium catenella* | AY347308 | AY347308 | AY347308 |
| *Ascogregarina taiwanensis* | EF666482 | EF666482 | EF666482 |
| *Babesia bigemina* | The Sanger Institute *Babesia bigemina* genome project (www.sanger.ac.uk/Projects/B_bigemina/) | | |
| *Bigelowiella natans* | U02075 | AF289036 | AF289036 |
| *Chromera velia* | DQ174731 | – | EU106870 |
| *Vitrella brassicaformis* | HM245049 | HM245049 | HM245049 |
| *Cryptosporidium parvum* | AF040725 | AF040725 | AF040725 |
| *Cylindrotheca closterium* | DQ082742 | AF289049 | AF289049 |
| *Eimeria tenella* | AF026388 | AF026388 | AF026388 |
| *Gonyaulax polyedra* | AF377944 | AF377944 | AF377944 |
| *Gregarina niphandrodes* | AF129882 | DQ837379 | DQ837379 |
| *Hyphochytrium catenoides* | X80344 | X80346 | X80345 |
| **Isospora belli* | – | DQ060683 | – |
| **Isospora felis* | L76471 | – | U85705 |
| **Mallomonas asmundae* | – | AF409122 | AF409122 |
| **Mallomonas striata* | M87333 | – | – |
| *Paramecium tetraurelia* | AF149979 | AF149979 | AF149979 |
| *Perkinsus atlanticus* | AF509333 | AF509333 | AF509333 |
| *Pfiesteria piscicida* | AY112746 | AY112746 | AY112746 |
| *Phytophthora megasperma* | M54938 | EF213612 | X75631 |
| *Plasmodium berghei* | M19712 | AJ298081 | AJ301624 |
| *Plasmodium falciparum* | M19172 | U21939 | U21939 |
| *Prorocentrum micans* | AY803739 | AF370878 | X16108 |
| **Sarcocystis canis* | – | DQ176645 | – |
| **Sarcocystis muris* | M64244 | – | AF012883 |
| **Spathidium amphoriforme* | – | AF223570 | AF223570 |
| **Spathidium sp.* | Z22931 | – | – |
| *Sterkiella histriomuscorum* | FJ545743 | FJ545743 | FJ545743 |
| *Theileria annulata* | KF429795 | KF429798 | JN696678 |
| *Theileria parva* | L02366 | AF218825 | AF218825 |
| *Toxoplasma gondii* | M97703 | X75453 | AF076901 |

*The alignment included sequences composed of genes from two closely related species.

### Molecular phylogenetic analyses

Three sets of alignments were used for phylogenetic analyses: SSU, LSU, and concatenated SSU, 5.8S, and LSU rDNA sequences: 1,604; 2,869, and 4,627 sites, respectively (after removing hypervariable regions and gaps). The alignments were constructed using MUSCLE 3.6 (Edgar 2004) and manually tuned with BioEdit 7.0.9.0 (Hall 1999). Ribosomal DNA sequences of heterokonts and rhizarians were used as outgroups. The taxonomic range was substantially limited by the available alveolate sequences of 5.8S and LSU rDNA. We managed to find just two gregarine LSU rDNA sequences: *Gregarina niphandrodes* and *Ascogregarina taiwanensis* (Toso and Omoto 2007, Templeton *et al*. 2010). To enhance the whole dataset, missing gene sequences for three outgroups (heterokonts, ciliates and coccidians) were taken from closely related species (i.e., representatives of the same genus or closely related genera, which are presented in GenBank). The rDNA sequences were tested to see if they localized in the same clusters (i.e. heterokonts, ciliates and coccidians), both in SSU and LSU phylogenetic analyses. Following this, the sequences were concatenated and added to ribosomal operon multigene alignment (Table 1). The use and validity of composite taxa in phylogenetic analysis has been previously discussed and applied earlier (Philippe *et al*. 2004, Leander and Keeling 2004, Delsuc *et al*. 2006, Bourlat *et al*. 2008, Campbell and Lapointe 2009).

For the SSU rDNA alignment, we preliminarily examined a large taxon sampling of alveolates (>300 OTUs, including majority of sequenced gregarine species), using certain features of predicted secondary structure of SSU rRNA during manual aligning, especially of problematic regions in gregarines: aligning using automatic software failed there. The resulting tree topology was compatible with previously published work (Rueckert *et al*. 2011b). We then removed a majority of the OTUs from the alignment, retaining the 31 OTUs for the phylogenetic analyses described below.

Maximum-likelihood (ML) analyses were performed with RAxML 7.2.8 (Stamatakis 2006) under GTR+Γ+I and GTR+Γ models, with 12 categories of discrete gamma distribution. The ML analyses included bootstraping with 1,000 replicates and 100 independent runs of ML each. Bayesian inference (BI) analysis was conducted using MrBayes 3.2.1 program (Ronquist and Huelsenbeck 2003), under a GTR+Γ+I model. The program was set to operate using the following parameters: nst = 6, ngammacat = 12, rates = invgamma, covarion = yes; parameters of Metropolis coupling Markov chains Monte Carlo (mcmc): nchains = 4, nruns = 2, temp = 0.2, ngen = 3,000,000, samplefreq = 1,000, burninfrac = 0.5 (first 50% of 3,000 sampled trees, i.e. first 1,500 ones, were discarded in each run). Standard deviation of split frequencies averaged 0.001 in the LSU rDNA analysis and of 0.002 in the concatenated ribosomal DNA analysis.

For SSU rDNA, two Bayesian analyses were performed on the 31 OTUs alignment: one with the same parameters as above (average standard deviation was 0.03) and another one with increased numbers of generations and independent runs (nruns = 8, ngen = 7,000,000). Standard deviation of split frequencies averaged 0.007. ML analysis was performed with the parameters specified above. In addition, we performed ML analyses of reduced alignments of SSU rDNA, where non-alveolate outgroups, and long-branch forming representatives (the crustacean gregarines, *Gregarina niphandrodes,* and *Plasmodium* spp.) were excluded; the parameters of the computations were the same as in the LSU rDNA and operon analyses. The topology, which is identical to that LSU rDNA and ribosome operon trees, was used as a constraint for branch lengths and node supports calculation in SSU rDNA trees under the same parameters. Topology tests for the 31 OTU Bayesian, ML, and user trees were performed using TREEFINDER (Jobb *et al*. 2004, Jobb 2011). For comparison of branch lengths in different trees and evaluation of molecular evolution rates, the measurements of the branch lengths were performed manually using scale bars.

## RESULTS

### Light microscopy (LM)

Solitary cells of *C.* cf. *communis* (Fig. 2A, B) demonstrated typical tricystid organization, since they are subdivided in three distinct compartments: small lenticular epimerite (according to the generic diagnosis in: Clopton 2000), protomerite, and deutomerite, which are separated from one another by two septa. The septa are more distinctly visible under DIC. Syzygies were not observed by us and therefore were not studied.

Solitary individuals and syzygy primites of *H.* cf. *longissima* (Fig. 2C, D) had similar tricystid organization with two septa, but syzygy satellites did not have an epimerite; therefore we classified them as dicystid. Unfortunately, DIC studies were impossible during the material collecting on Lake Baikal.

### Transmission electron microscopy (TEM)

#### *Cephaloidophora* cf. *communis* (Fig. 3)

The cross-sections through the middle of the cell demonstrated a typical eugregarine tegument structure: a trimembrane pellicle (~30 nm thick) covered by a cell coat (~10 nm thick), forming numerous epicytic folds (Fig. 3A–C). Cross-sections of the folds show a finger-like shape: they have parallel lateral sides and slightly swollen rounded tops. The height of the folds significantly varies from ~400 nm in the middle of the body to ~260 nm (and probably less) closer to the anterior end of the cell, while the thickness of the folds remains the same and averages ~130 nm (tops) and ~100 nm (stems). There are three distinct apical arcs in the fold tops and two apical filaments, which are very difficult to detect; however, it is possible to discern them in some photos (Fig. 3B, C). The two apical filaments face spaces between the three apical arcs (they are not in front of apical arcs themselves). Beneath the pellicle is a layer (35 nm thick) forming crossbars at the bases of the folds (Fig. 3B). Micropores are located at

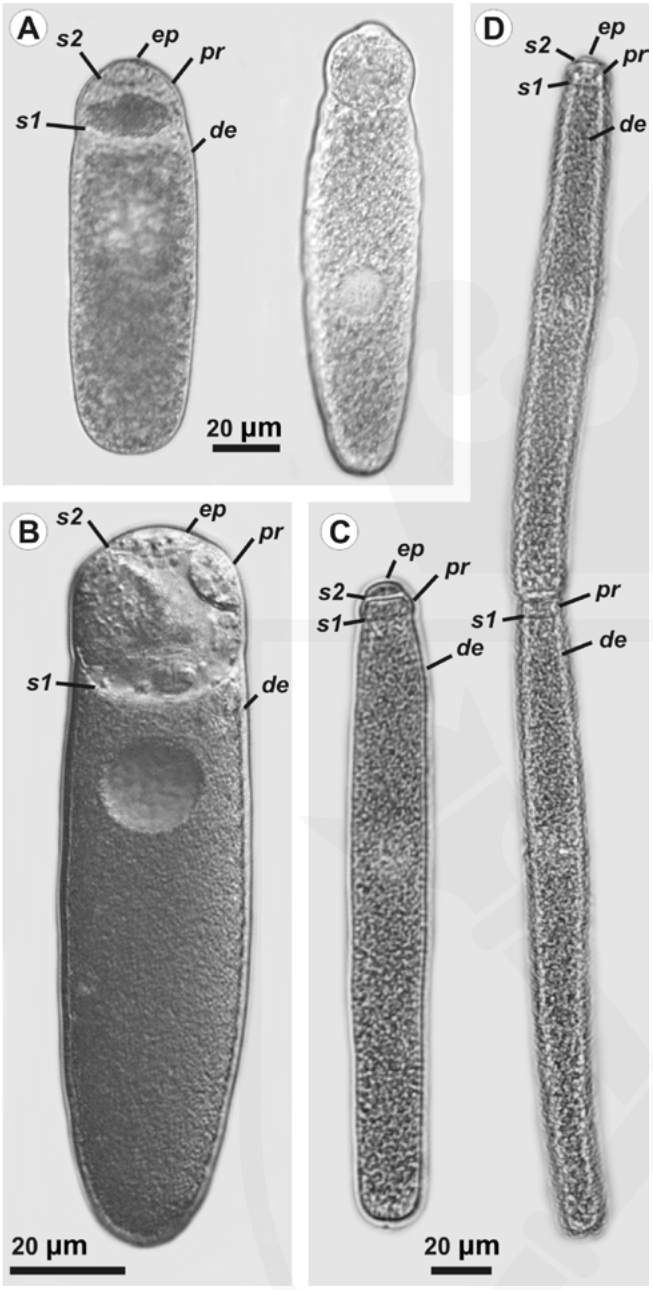


**Fig. 2.** Light microscopy of the gregarine studied: free individuals (gamonts) of *Cephaloidophora* cf. *communis* (**A**, common light microsopy; **B**, DIC microscopy); a free gamont (**C**) and a syzygy (**D**) of *Heliospora* cf. *longissima.* Epimerite (***ep***), promerite (***pr***), deutomerite (***de***), septum between poto- and deutomerite (***s1***), and septum between proto- and epimerite (***s2***) are visible.

the bottom of the grooves between the folds (Fig. 3B), without any regular pattern.

The cytoplasm is subdivided into ecto- and endoplasm. This stratification in gregarines is caused by the absence or presence of storage carbohydrate (amylopectin) grains, respectively (Vivier 1968). The thickness of the ectoplasm, free of amylopectin grains, was about 1 µm. The endoplasm contains numerous amylopectin grains, rounded shape up to 0.7 µm in diameter (Fig. 3A). The cytoplasm also contained numerous vacuoles with dense inclusions.

Longitudinal sections of the cell demonstrated two distinct septa: one between the epi- and protomerite and another between the proto- and deutomerite (Fig. 3D, E, G–I). Both septa appear to be fibrillar in nature (Fig. 3G, H, I). No contacts were observed between the septa and the pellicle (Fig. 3H). The anterior and middle parts of epimerite are filled by unusual objects, which look similar to micronemes (typically absent in gregarine trophozoites and gamonts) and tightly adjoin one another (Fig. 3F). There are pores in the epimerite pellicle previously observed by SEM (Rueckert *et al*. 2011b). Probably, the homogenous content of the microneme-like objects can be released through these pores (Fig. 3F). The posterior part of the epimerite cytoplasm comprises electron-translucent vacuoles (Fig. 3H). The protomerite cytoplasm has a foam-like structure (Fig. 3G, H, I), possibly formed by highly developed endoplasmic reticulum. Additionally, there are lipid drops and amylopectin grains in the middle and in the rear part of the protomerite (Fig. 3E). The number of these inclusions increased towards the posterior, and were in particularly high abundance in the deutomerite (Fig. 3D, E).

***Heliospora* cf. *longissima* from *Eulimnogammarus verrucosus* (Fig. 4).**

The transversal and longitudinal sections were studied. Unfortunately, the fixation was not very successful, and these samples could not be recollected. The cross-sections demonstrated pellicular epicytic club-shaped folds with swollen tops containing about 5 apical filaments and 4–6 hardly discernible apical arcs (Fig. 4A, B). The apical filaments face spaces between the apical arcs rather than the apical arcs themselves. The height of the folds varies from ~260 to ~500 nm, depending on location of the section: closer to the posterior end of the cell the folds are significantly lower than in the middle of the body, while the thickness remains the same (~140 nm tops and ~90 nm stems). Micropores were not observed. The subjacent layer of the pellicle was well developed, however, unlike *C*. cf. *communis* it is less electron-dense; its thickness was about 45 nm. The subdivision of the cytoplasm into ecto- and endoplasm

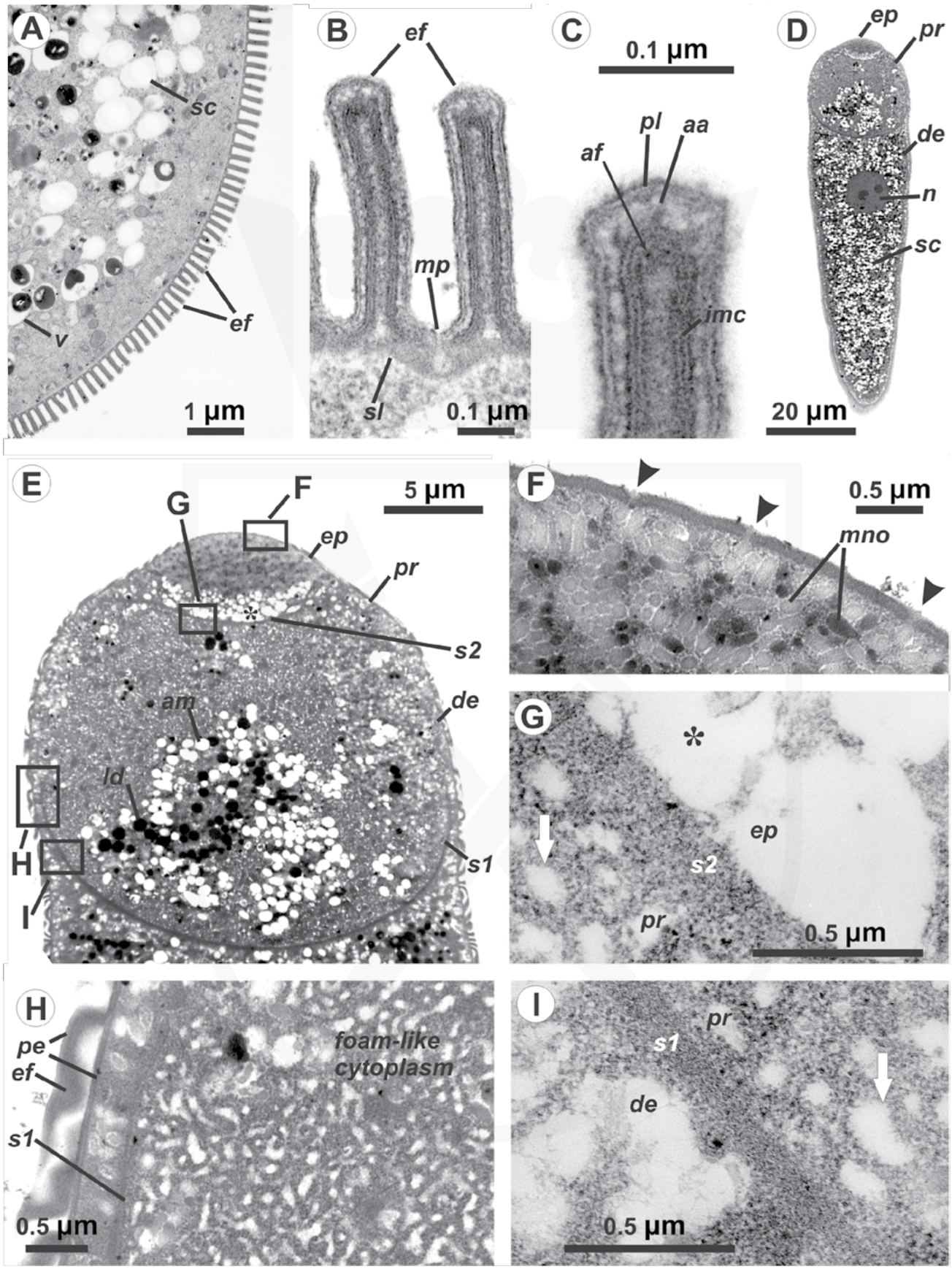
A
sc
v
ef
1 µm
B
ef
mp
sl
0.1 µm
C
0.1 µm
pl
aa
af
imc
D
ep
pr
de
n
sc
20 µm
E
5 µm
G
F
ep
pr
s2
am
de
ld
H
I
s1
F
0.5 µm
mno
G
ep
s2
pr
0.5 µm
H
pe
ef
s1
foam-like
cytoplasm
0.5 µm
I
pr
s1
de
0.5 µm

was not observed. Large (up to 0.75 μm) carbohydrate granules come close to the subjacent layer under the pellicle.

The longitudinal sections of the two separated syzygy partners, primite and satellite, were also studied (the syzygy was fragmented during the embedding procedure). The primite demonstrates differences of cytoplasm structure between its epimerite, protomerite, and deutomerite (Fig. 4C), despite the section missing the very apex of the cell. Just basal part of epimerite is present on the section; its cytoplasm looks homogeneous and does not contain any organelles or inclusions. A distinct septum between the epi- and protomerite is apparently absent (Fig. 4C). The protomerite cytoplasm is subdivided into two zones: anterior and posterior. The anterior zone looks darker and more homogeneous; the posterior zone is lighter and apparently contains many membranous structures (Fig. 4D, E). The protomerite contains large electron-dense globules (Fig. 4C, D), which are arranged mainly near its approximate anterior and posterior borders. However, several ones may be observed in the middle part. Such globules in the deutomerite as well, and they also occur near the deuto-/ protomerite interface, which may be observed as a (barely) visible, loose septum presumably consisting of thin fibrils (Fig. 4E). There are many large amylopectin granules within the deutomerite, unlike the epimerite and protomerite.

The fine structure of the satellite forebody sharply differs from that of primite. There is no epimerite. The protomerite is separated from the deutomerite by a thick granulated (or fibrillar) zone of the cytoplasm, which looks like a septum. The protomerite of the satellite contains no amylopectin grains, while the deutomerite is rich with them. The protomerite of the satellite is highly vacuolated. The vacuoles are large, electron-light, and contain large electron-dense globules (Fig. 4F, G).

**Molecular phylogeny**

ML analyses for all genes was conducted under GTR+Γ and GTR+Γ+I models. No significant changes were observed between these two models. The tree topologies were the same and the bootstrap supports varied only slightly (data not shown). Accordingly, one model, GTR+Γ+I, was used in the Bayesian analyses. The results presented below were obtained using this model only.

**Analyses of LSU rDNA and ribosomal operon (Fig. 5)**

Internal transcribed spacers (ITS1 and ITS2), 5.8S, and LSU rDNA sequences of both *Heliospora* cf. *longissima* samples (from *Eulimnogammarus verrucosus* and *E. vittatus*) were almost identical throughout their length (two substitutions out of the 2,833 included nucleotide sites for each sample). This confirms that the same gregarine species was present in two crustacean hosts. The phylogenetic trees were constructed using Bayesian Inference (BI) and Maximum Likelihood (ML) with bootstrapping for two datasets containing the same 31 OTUs. All the constructed trees had identical topologies, independent of the inference method. The apicomplexan clade comprised chromerids and sporozoans, the latter included the clades of cryptosporidia+gregarines and coccidians+hematozoans. The trees contain the long branches of *Plasmodium* spp., *Gregarina niphandrodes*,

◀◀

**Fig. 3.** Ultrastructure of the gregarine *Cephaloidophora* cf. *communis* on transverse (**A**–**C**) and longitudinal (**D**–**I**) sections. **A**, a fragment of a cross section showing the cytoplasm with grains of amylopectin (***am***) and epicytic folds (***ef***); **B**, a micropore (***mp***) between two epicytic folds; **C**, an epicytic fold structure (***pl***, plasmalemma (plasma membrane with cell coat); ***imc*,** internal membrane complex; ***aa***, apical arcs; ***af***, apical filaments; ***sl***, subjacent layer); **D**, a longitudinal section of a trophozoite showing an epimerite (***ep***), a protomerite (***pr***), and a deutomerite (***de***), which contains nucleus (***n***) and a lot of amylopectin grains (***am***); **E**, anterior part of the same section: the rectangles mark areas shown on **F, G**, **H** and **I** (***s1***, a regular protomerite/ deutomerite septum; ***s2***, a protomerite/ epimerite septum; ***ld***, lipid drops; ***am***, amylopectin grains), note that posterior part of the epimerite (***ep***) contains large electron translucent vacuoles (asterisk, also on **G**), whereas its middle and anterior parts are electron dense; **F**, the anterior and middle parts of the epimerite are full of microneme-like objects (***mno***) probably capable to secrete their content through putative pores in the pellicle, which sometimes look as being connected with these objects (arrowheads); **G**, the septum (***s2***) separating posterior of the epimerite (***ep***), containing electron-translucent vacuoles marked by the asterisk, and the protomerite (***pr***), cytoplasm of which has foam-like structure: the arrow marks a separate "bubble" of this foam; **H**, foam-like cytoplasm of protomerite and beginning of the protomerite/deutomerite septum (***s1***) in its cortical zone, which contacts the pellicle (***pe***) in neither basal nor apical parts of the epicityc folds (***ef***) but goes parallel to it; **I**, septum (***s1***) separating the protomerite (***pr***) and deutomerite (***de***) cytoplasm; arrow is the same that on **G**.

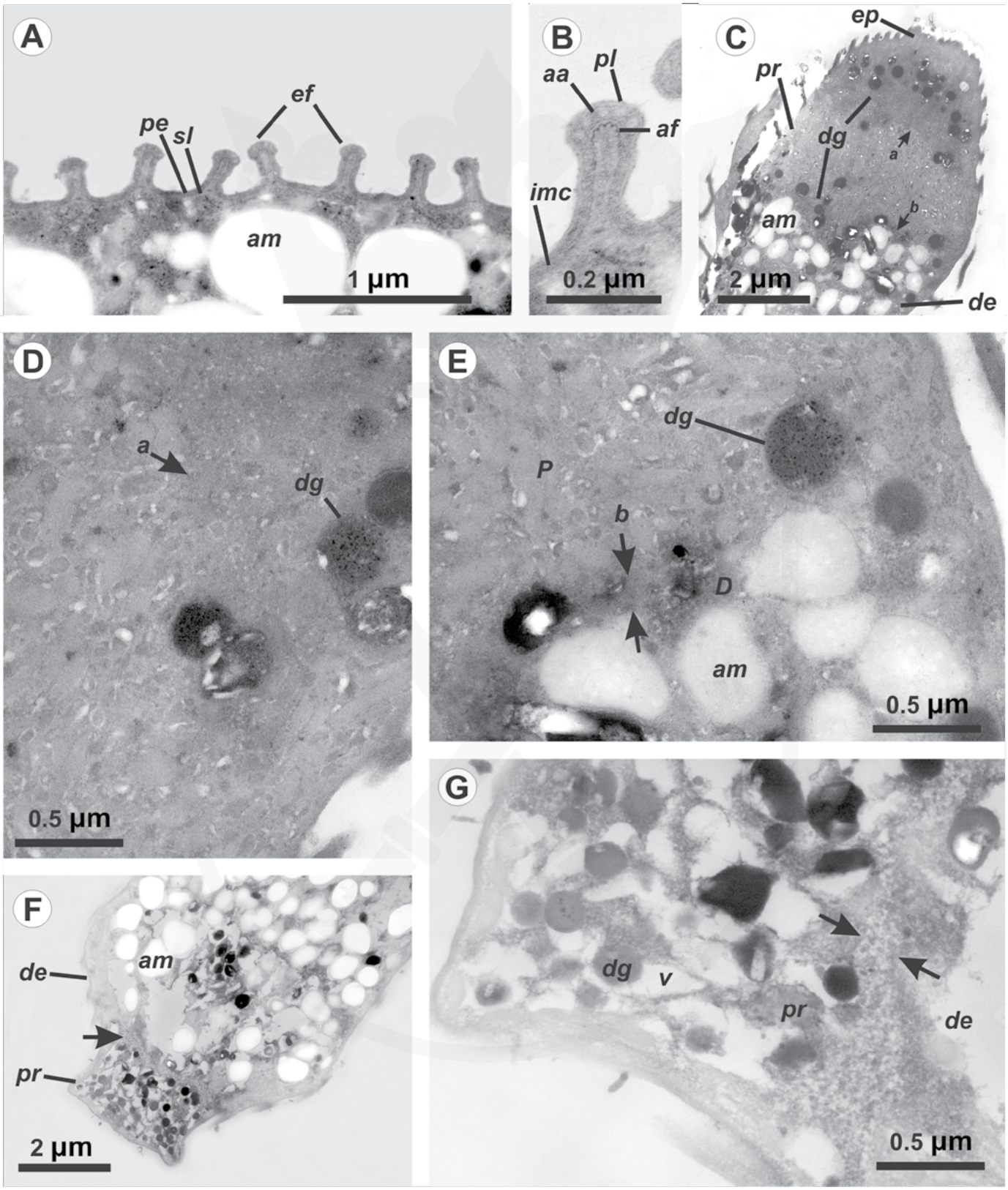
A
pe
sl
ef
am
1 µm
B
aa
pl
af
imc
0.2 µm
C
ep
pr
dg
a
b
am
2 µm
de
D
a
dg
0.5 µm
E
dg
P
b
D
am
0.5 µm
F
de
am
pr
2 µm
G
dg
v
pr
de
0.5 µm

and the two gregarines in this study parasitizing crustacean hosts, *Cephaloidophora* cf. *communis* and *Heliospora* cf. *longissima*.

In the LSU tree (Fig. 5A), most alveolate clades were highly supported in both Bayesian (PP = 0.95–1.0) and ML analysis (BP = 95–100%). The only exception was the clade containing all gregarines with PP = 0.92 and BP = 56%. The clades of chromerids, and of cryptosporidians + gregarines, were highly supported by Bayesian analyses, but moderately supported by ML analyses (PP = 0.95 and 1.0, and BP = 76% and 88%, respectively). Three sequences from the Cephaloidophoroidea formed a robust clade with full support of both Bayesian and ML analyses. This clade grouped with another long branch, *Gregarina niphandrodes,* with high support (PP = 1, BP = 95%).

In the ribosomal operon tree (Fig. 5B), the support values were similar to the LSU tree, but the gregarine clade had a higher PP (1.0 instead of 0.92) and BP (71% instead of 56%). However, support for the long branches of *G. niphandrodes* and Cephaloidophoroidea, the BP value decreased from 95% in LSU rDNA tree to 85%.

**Analyses of SSU rDNA (Fig. 6)**

In order to obtain comparable results, we analyzed SSU rDNA for the same sample of 31 OTUs. Bayesian and ML analyses yielded different results. The topology of the Bayesian consensus tree (Fig. 6A) was similar to those of the LSU rDNA and ribosomal operon trees; the only exception being chromerids, which appeared at the base of dinoflagellates, and the branch containing the Cephaloidophoroidea. The Cephaloidophoroidea grouped with coccidians, rather than with other gregarines. Nodal support at deeper positions within the tree had low resolution, although the support values for the Myzozoa clade, ciliates, as well as for alveolates, as a whole, were high. The increased number of generations or independent runs had no effect on the support values (data not shown).

The ML tree of 31 OTUs does not correspond to the current views on alveolate phylogeny (i.e., the relationship between dinoflagellate and apicomplexan clades was poorly supported). Support for many of the subgroups within these larger clades was also uncertain in our analyses. Chromerids appeared within the dinoflagellate clade, as well as a clade containing gregarines and cryptosporidians. The Cephaloidophoroidea had low support at the tip of dinoflagellates.

In order to evaluate the influence of long branch attraction (LBA), we sequentially removed non-alveolate outgroups and each long branch from the alignment (*Plasmodium* spp, *Gregarina niphandrodes*, and crustacean gregarines), as recommended by Bergsten (2005), and recalculated the ML trees each time, however this did not yield any improvement or result in a considerable change to the tree topology (data not shown).

Because of inconsistency is present in the Bayesian and ML SSU rDNA tree topologies, as well as discrepancy between those and LSU rDNA and ribosomal operon trees, we tested all three topologies (Figs 5 and 6), including a constraint SSU rDNA tree. The constraint SSU rDNA tree had the same branching order as both the LSU rDNA and ribosomal operon trees. None of the topology tests rejected any of these topologies (Table 2). This means that the LSU rDNA and ribosomal operon tree topology is also valid for SSU rDNA phylogeny of the 31 OTUs; although, it was not elected by the programs as a topology of "the best tree", in this case.

Additional to the topology testing, we compared PP and BP supports of main clades in the three trees that shared the same topology (i.e., the constraint SSU rDNA tree and the trees resulting from the LSU rDNA and ri-

◀◀

**Fig. 4.** Ultrastructure of the gregarine *Heliospora* cf. *longissima* on transverse (**A, B**) and longitudinal (**C–G**) sections. **A**, a fragment of a cross section showing the cytoplasm with grains of storage carbohydrate (***sc***) and epicytic folds (***ef***), the subjacent layer (***sl***) is visible; **B**, structure of an epicytic fold (***pl***, plasmalemma (plasma membrane with cell coat); ***imc*,** internal membrane complex; ***aa***, apical arcs; ***af***, apical filaments; ***sl***, subjacent layer; **C**, a longitudinal section of the anterior part of a primite (anterior syzygy partner) showing the epimerite (***ep***), the protomerite (***pr***), and the deutomerite (***de***); note dense globules (***dg***) in the protomerite near its borders; the arrow ***a*** marks the border between anterior and posterior parts of the protomerite, the arrow b marks the proto- / deutomerite border; **D**, the border (arrow "a" corresponds to arrow "a" on **C**) separating protomerite cytoplasm; ***dg***, dense globules; **E**, a weak septum (arrows, the arrow "b" corresponds to arrow "b" on **C**) separating the protomerite (***pr***) and deutomerite (***de***) cytoplasm; **F**, a longitudinal section of the anterior part of a satellite (posterior syzygy partner) showing protomerite (***pr***), deutomerite ***(de),*** and a thick septum between them (arrow)**;** **G**, part of the same under higher magnification (***dg***, dark granules, ***v***, vacuoles).

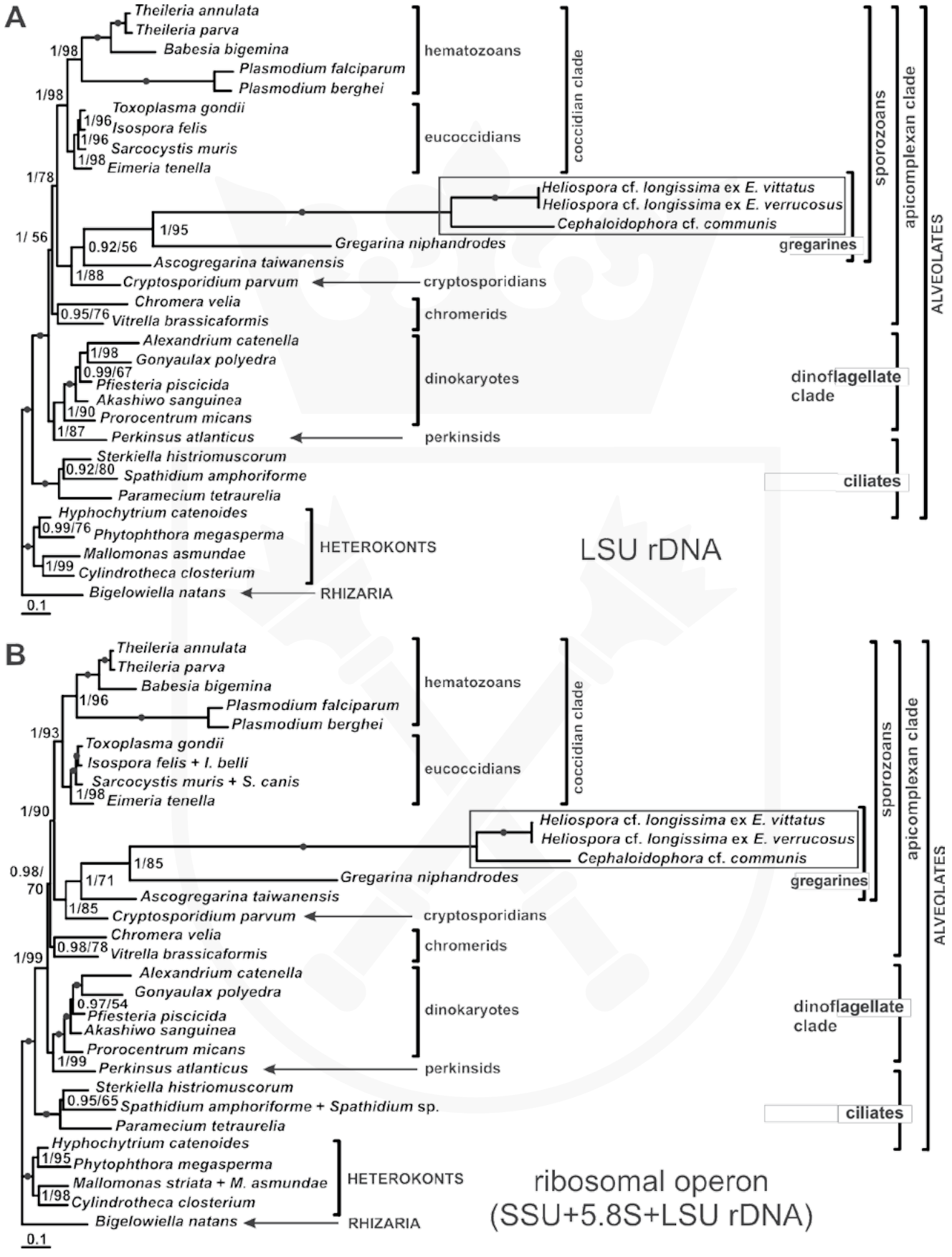
A
Theileria annulata
Theileria parva
Babesia bigemina
Plasmodium falciparum
Plasmodium berghei
Toxoplasma gondii
Isospora felis
Sarcocystis muris
Eimeria tenella
Heliospora cf. longissima ex E. vittatus
Heliospora cf. longissima ex E. verrucosus
Cephaloidophora cf. communis
Gregarina niphandrodes
Ascogregarina taiwanensis
Cryptosporidium parvum
Chromera velia
Vitrella brassicaformis
Alexandrium catenella
Gonyaulax polyedra
Pfiesteria piscicida
Akashiwo sanguinea
Prorocentrum micans
Perkinsus atlanticus
Sterkiella histriomuscorum
Spathidium amphoriforme
Paramecium tetraurelia
Hyphochytrium catenoides
Phytophthora megasperma
Mallomonas asmundae
Cylindrotheca closterium
Bigelowiella natans
1/98
1/98
1/96
1/96
1/98
1/78
1/ 56
1/95
0.92/56
1/88
0.95/76
1/98
0.99/67
1/90
1/87
0.92/80
0.99/76
1/99
0.1
hematozoans
eucoccidians
coccidian clade
gregarines
cryptosporidians
chromerids
dinokaryotes
perkinsids
HETEROKONTS
RHIZARIA
sporozoans
apicomplexan clade
dinoflagellate clade
ciliates
ALVEOLATES
LSU rDNA
B
Theileria annulata
Theileria parva
Babesia bigemina
Plasmodium falciparum
Plasmodium berghei
Toxoplasma gondii
Isospora felis + I. belli
Sarcocystis muris + S. canis
Eimeria tenella
Heliospora cf. longissima ex E. vittatus
Heliospora cf. longissima ex E. verrucosus
Cephaloidophora cf. communis
Gregarina niphandrodes
Ascogregarina taiwanensis
Cryptosporidium parvum
Chromera velia
Vitrella brassicaformis
Alexandrium catenella
Gonyaulax polyedra
Pfiesteria piscicida
Akashiwo sanguinea
Prorocentrum micans
Perkinsus atlanticus
Sterkiella histriomuscorum
Spathidium amphoriforme + Spathidium sp.
Paramecium tetraurelia
Hyphochytrium catenoides
Phytophthora megasperma
Mallomonas striata + M. asmundae
Cylindrotheca closterium
Bigelowiella natans
1/96
1/93
1/90
0.98/ 70
1/71
1/85
1/85
0.98/78
1/99
0.97/54
1/99
0.95/65
1/95
1/98
0.1
hematozoans
eucoccidians
coccidian clade
gregarines
cryptosporidians
chromerids
dinokaryotes
perkinsids
HETEROKONTS
RHIZARIA
sporozoans
apicomplexan clade
dinoflagellate clade
ciliates
ALVEOLATES
ribosomal operon
(SSU+5.8S+LSU rDNA)

bosome operon analyses) (Table 3). The higher support values tended to coincide with increasing the amount of sites included in the analyses. This trend was especially apparent in the apicomplexan clades, and clades containing their close relatives, chromerids. Support values for clades based on LSU rDNA were considerably higher than those based on SSU rDNA. The clade containing the Cephaloidophoroidea clade was robust throughout all three trees. It was also noticed that PP values were higher than BP values in each case.

Finally, we compared rates of molecular evolution in LSU and SSU rDNA among apicomplexans using branch lengths. For this, branch lengths of apicomplexan OTUs were measured using scale bars from the root (common ancestor) of sporozoans (parasitic apicomplexans) to the leaves (tips) in the Bayesian trees of identical topologies: SSU rDNA constraint, LSU rDNA, and ribosomal operon trees. The branch length values (absolute evolutionary rates) were expressed in substitutions/site (Table 4).

**Table 2.** Results of SSU rDNA tree topology tests.

| Tree topology | – ln L | bp[a] | ELW[b] | kh[c] | sh[d] | WSH[e] | AU[f] |
|---|---|---|---|---|---|---|---|
| Fig. 6A (Bayesian) | 17158.31 | 0.261015 | 0.2628862 | 0.401667 | 0.607025 | 0.617512 | 0.5124509 |
| Fig. 6B (ML) | 17155.49 | 0.51943 | 0.5164639 | 1.0 | 1.0 | 1.0 | 0.6466904 |
| as on Fig. 5 (constraint[g]) | 17160.78 | 0.219555 | 0.2204883 | 0.333012 | 0.444848 | 0.475636 | 0.3695847 |

[a] Bootstrap Probability (Felsenstein 1985); [b] Expected-Likelihood Weights (Strimmer and Rambaut 2002); cp-value of the Kishino-Hasegawa test (Kishino and Hasegawa 1989); dp-value of the Shimodaira-Hasegawa test (Shimodaira and Hasegawa 1999); dp-value of the Weighted Shimodaira-Hasegawa Test (Shimodaira and Hasegawa 1999); fP-value of the Approximately Unbiased test (Shimodaira 2002); gconstraint according to the LSU rDNA / ribosome operon tree topology. $P < 0.05$ discards current topology.

**Table 3.** Posterior probability (PP) and bootstrap percentage (BP) support of main clades in the SSU rDNA, LSU rDNA, and ribosomal operon trees*.

| Clade | SSU rDNA constraint tree (PP/BP) | LSU rDNA tree (PP/BP) | Ribosomal operon tree (PP/BP) |
|---|---|---|---|
| Alveolates | 1/98 | 1/100 | 1/100 |
| Ciliates | 1/99 | 1/100 | 1/100 |
| Myzozoa | 1/69 | 1/100 | 1/99 |
| Dinoflagellate (including perkinsids)** | 0.93/48 | 1/87 | 1/99 |
| Apicomplexans (including chromerids)** | 0.02/11 | 1/56 | 98/70 |
| Chromerids** | 0.08/14 | 0.95/76 | 98/78 |
| Sporozoans** | 0.56/17 | 1/76 | 1/90 |
| Coccidian clade (including hematozoans) | 0.50/57 | 1/98 | 1/93 |
| Gregarine clade** | 0.41/23 | 0.92/56 | 1/71 |
| Crustacean gregarines | 1/100 | 1/100 | 1/100 |

* All the three trees have the same topology of resulting tree from LSU and/or ribosomal operon analysis (Fig. 5).
** The clades are absent on the SSU rNA RAxML best tree.

**Fig. 5.** Bayesian inference (BI) trees of alveolates constructed using the GTR+Γ+I model for 31 OTUs: **A**, LSU rDNA; **B**, ribosome operon. Numbers at the nodes indicate Bayesian posterior probabilities (numerator) and ML bootstrap percentage (denominator). Black dots on the branches indicate Bayesian posterior probabilities and bootstrap percentages of 1 and 100%, respectively. The gregarines from crustacean hosts are framed.

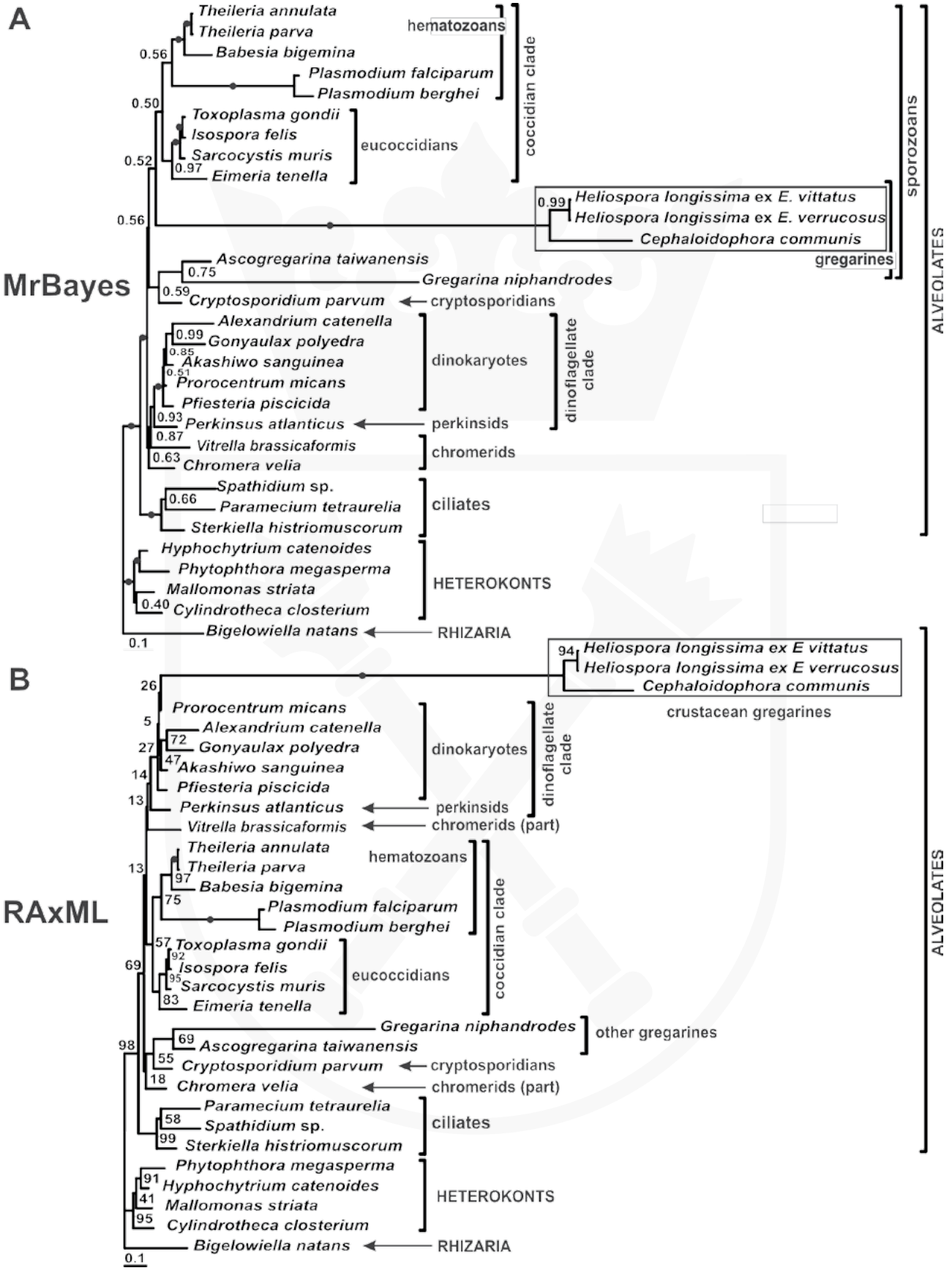
A
MrBayes
Theileria annulata
Theileria parva
Babesia bigemina
Plasmodium falciparum
Plasmodium berghei
hematozoans
coccidian clade
Toxoplasma gondii
Isospora felis
Sarcocystis muris
Eimeria tenella
eucoccidians
Heliospora longissima ex E. vittatus
Heliospora longissima ex E. verrucosus
Cephaloidophora communis
gregarines
sporozoans
ALVEOLATES
Ascogregarina taiwanensis
Gregarina niphandrodes
Cryptosporidium parvum
cryptosporidians
Alexandrium catenella
Gonyaulax polyedra
Akashiwo sanguinea
Prorocentrum micans
Pfiesteria piscicida
dinokaryotes
dinoflagellate clade
Perkinsus atlanticus
perkinsids
Vitrella brassicaformis
Chromera velia
chromerids
Spathidium sp.
Paramecium tetraurelia
Sterkiella histriomuscorum
ciliates
Hyphochytrium catenoides
Phytophthora megasperma
Mallomonas striata
Cylindrotheca closterium
HETEROKONTS
Bigelowiella natans
RHIZARIA
B
RAxML
Heliospora longissima ex E vittatus
Heliospora longissima ex E verrucosus
Cephaloidophora communis
crustacean gregarines
Prorocentrum micans
Alexandrium catenella
Gonyaulax polyedra
Akashiwo sanguinea
Pfiesteria piscicida
dinokaryotes
dinoflagellate clade
Perkinsus atlanticus
perkinsids
Vitrella brassicaformis
chromerids (part)
Theileria annulata
Theileria parva
Babesia bigemina
Plasmodium falciparum
Plasmodium berghei
hematozoans
coccidian clade
Toxoplasma gondii
Isospora felis
Sarcocystis muris
Eimeria tenella
eucoccidians
Gregarina niphandrodes
other gregarines
Ascogregarina taiwanensis
Cryptosporidium parvum
cryptosporidians
Chromera velia
chromerids (part)
Paramecium tetraurelia
Spathidium sp.
Sterkiella histriomuscorum
ciliates
Phytophthora megasperma
Hyphochytrium catenoides
Mallomonas striata
Cylindrotheca closterium
HETEROKONTS
Bigelowiella natans
RHIZARIA
ALVEOLATES

**Table 4.** Rates of molecular evolution (substitutions/site) of apicomplexans as calculated in SSU rDNA, LSU rDNA, and ribosomal operon phylogenetic analyses.

| Branch | SSU rDNA constraint tree* | LSU rDNA tree | Ribosomal operon tree |
|---|---|---|---|
| Cryptosporidium parvum | 0.11 | 0.23 | 0.16 |
| Ascogregarina taiwanensis | 0.21 | 0.33 | 0.29 |
| Gregarina niphandrodes | 0.90 | 0.98 | 1.02 |
| *Heliospora* cf. *longissima* ex *Eulimnogammarus vittatus* | 1.51 | 1.73 | 1.72 |
| *Heliospora* cf. *longissima* ex *E. verrucosus* | 1.51 | 1.73 | 1.72 |
| *Cephaloidophora* cf. *communis* | 1.70 | 1.79 | 1.86 |
| Isospora** | 0.09 | 0.10 | 0.10 |
| Toxoplasma gondii | 0.09 | 0.10 | 0.10 |
| Sarcocystis*** | 0.09 | 0.10 | 0.10 |
| Eimeria tenella | 0.16 | 0.12 | 0.14 |
| Babesia bigemina | 0.18 | 0.35 | 0.30 |
| Theileria parva | 0.12 | 0.27 | 0.22 |
| Theileria annulata | 0.12 | 0.26 | 0.21 |
| Plasmodium berghei | 0.54 | 0.63 | 0.63 |
| Plasmodium falciparum | 0.49 | 0.63 | 0.60 |

* The SSU rDNA constraint tree has the same topology as the LSU rDNA and ribosomal operon trees (Fig. 5); the branch lengths (from the common ancestor of sporozoans to the leaves) were calculated with the MrBayes program.
** SSU and LSU rDNAs of *Isospora felis*, 5.8 rDNA of *I. belli*.
*** SSU and LSU rDNAs of *Sarcocystis muris*, 5.8 rDNA of *S. canis*.

Comparing individual branch lengths (Table 4), the long-branching species have just slightly longer branches in the LSU rDNA than in the SSU rDNA tree (~1.12 times). For the non-long-branching apicomplexans, the situation is more complicated. Species with moderate branch lengths (*Cryptosporidium, Ascogregarina, Babesia,* and *Theileria* spp.) have branches of about 1.5–2.5 (~2 on average) times longer in the LSU than the SSU rDNA tree. The shortest branches of coccidians keep the same lengths or are even a bit shorter. The average branch lengths of the nine non-long-branching or "slow-evolving" apicomplexans ($S_a$ = total branch length of the four coccidians, three hemosporidians (without *Plasmodium* spp.), *Cryptosporidium*, and *Ascogregarina*, divided by 9) were equal to ~0.13 and ~0.21 substitutions/site for SSU and LSU rDNA, respectively.

Branch length pattern of the LSU rDNA tree considerably differs from that of the SSU rDNA trees, including the constraint SSU rDNA tree of the same topology. Despite the absolute evolutionary rates of apicomplexan LSU rDNA being higher than SSU rDNA, the long branches in the former look relatively shorter, if to compare with the non-long-branching apicomplexans (Figs 5 and 6). Therefore, we calculated *relative* evolutionary rates for each long branch (*G. niphandrodes*, *C.* cf. *communis*, *H.* cf. *longissima* samples, and two *Plasmodium* species) as a ratio $L / S_{a,}$ where L = length

**Fig. 6.** Two different trees of alveolates inferred by different methods using the GTR+Γ+I model for the same alignment of SSU rDNA sequences for 31 OTUs: **A**, Bayesian inference (BI), MrBayes program; **B**, maximum likelihood (ML), RAxML program. Numbers at the nodes indicate Bayesian posterior probabilities (in **A**) or ML bootstrap percentage (in **B**). Black dots on branches indicate Bayesian posterior probabilities or bootstrap percentages of 1 and 100%, respectively. The gregarines from crustacean hosts marked by rectangles. Note that both methods failed to establish the admissible positions of the crustacean gregarines and some other alveolate clades here, but the BI tree shows better results.

of a certain long branch (e.g. *C.* cf. *communis*) and $S_a$ = averaged branch length of the nine non-long-branching apicomplexans (see above). Our results showed that the relative evolutionary rates of the long-branching apicomplexans LSU rDNA are approximately 1.5 times less than the relative evolutionary rates of their SSU rDNA (Fig. 7).

Apicomplexan branch lengths in the ribosome operon tree (Table 4) appeared to be between SSU and LSU rDNAs branch lengths, with the exception of the long-branching species (i.e., *Plasmodium* spp. and the gregarines *C.* cf. *communis*, *H.* cf. *longissima,* and *G. niphandrodes*) which have branches of the same length, or even somewhat longer (*C.* cf. *communis*) than those in the LSU rDNA tree. The 5.8S rDNA region in these species is likely a contributing factor. This region is extremely variable in these species, compared to other OTUs.

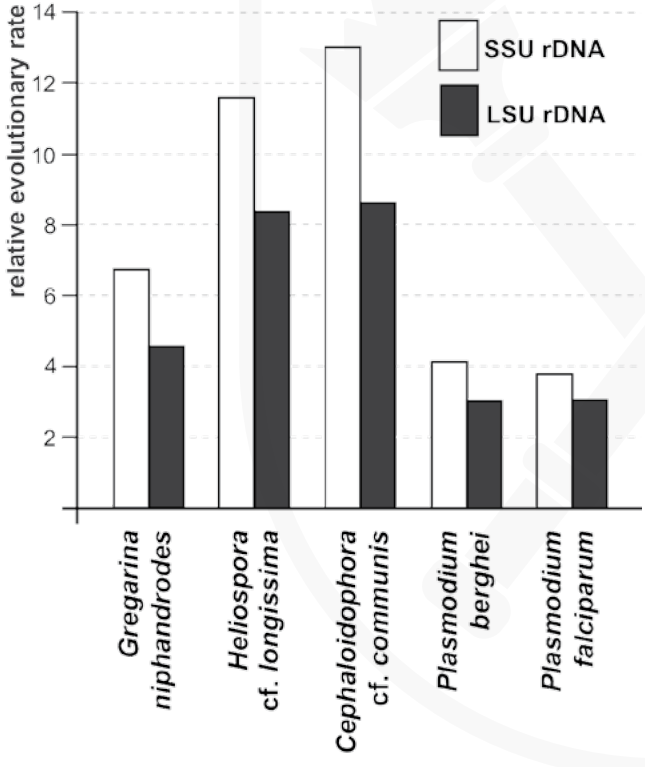


**Fig. 7.** Relative rates of molecular evolution in long-branch apicomplexans: SSU rDNA (white columns) and LSU rDNA (black columns), calculated as ratio of the length of the current branch to average branch length of the non-long-branch apicomplexans (see the text for more explanations). Relative rates of LSU rDNA evolution are lower than those of SSU rDNA, especially in gregarines.

## DISCUSSION

### Remarks on phylogenetic analyses

SSU rDNA sequences from different sporozoans evolve at highly heterogeneous rates. Notably, gregarines form long branches on phylogenetic trees, especially gregarines from crustaceans (Cephaloidophoroidea). For this reason, the trees comprising such clades may be affected by long branch attraction (LBA) (see review of J. Bergsten 2005). Apart from LBA, high rates of evolution in SSU rDNA (e.g., high amounts of insertions and deletions (indels) and subsitutions) are characteristic, even for those regions of gregarine SSU rDNA, which are only moderately variable in other eukaryotes. Such regions are the most important for phylogenetic analyses, since they obviously contain pronounced phylogenetic signal. The large amount of indels and substitutions also makes alignment of these regions difficult or impossible. For these reasons, long-branching lineages, such as cephaloidophoroid gregarines, as well as other groups of gregarines, are "rogue" taxa.

The 31 OTU trees based on SSU rDNA alone were inconsistent with (i) each other, (ii) a previously published study of 82 OTU alignment, comprising the crustacean gregarines (Rueckert *et al*. 2011b), and (iii) phylogenetic inferences from our preliminary analysis of the large taxon sampling. Moreover, these results did not fit expectations from morphological data. Both the trees demonstrated distorted topologies and many nodes had low support. From this, we can conclude that the reduction in sample size of SSU rDNA to 31 OTUs exerted a distinctly negative influence on the results of SSU rDNA analyses. We can also conclude that ML analyses yielded a less accurate inference, compared to the Bayesian approach, which proved to be less sensitive to size changes of taxon sampling. For example, in the ML tree topology, there is no clade uniting all sporozoans (parasitic apicomplexans) and the crustacean gregarines affiliated with dinoflagellates. In this case other gregarines, chromerids, and *Cryptosporidium,* became a sister group to all other Myzozoa (dinoflagellates + coccidians), whereas, in the Bayesian tree, the sporozoan clade exists, and the crustacean gregarines are situated within this clade. These findings fit the empiric results of Alfaro *et al*. (2003), which concluded (i) that the Bayesian approach is more susceptible to phylogenetic signal, (ii) it is a less biased predictor of phylogenetic accuracy than ML-bootstrapping method,

and (iii) it provides high support values for correct topological bipartitions with fewer characters than was needed for nonparametric bootstrap.

PP nodal support tends to be considerably higher than BP in the majority of the clades in our trees. This phenomenon was previously mentioned, along with the limited correlation between PP and BP values. (Alfaro *et al*. 2003, Cummings *et al*. 2003, Douady *et al*. 2003, Erixon *et al*. 2003). These values supply different aspects to a phylogenetic analysis. Alfaro *et al*. (2003) concluded that high Bayesian PP can indicate that the node is indeed correct; however, this was a condition based on the data set and the model of evolution. Moderate BP support of the nodes could indicate a high dependence on the underlying composition of the data matrix (i.e., taxon and gene sampling). Thus, increasing the amount of data used in the analyses, could result in either the disappearance of an artifactual node, or, conversely, the consistency of the node will increase (BP support will become higher), if the node is correct. In our study, we have the observed the latter case for majority of apicomplexan clades in Bayesian SSU, LSU, and concatenated rDNA trees. Therefore, we conclude that phylogenetic analysis employing Bayseian methodologies are the preferred method of inferring phylogenetic relationships among apicomplexans.

The 31 OTU SSU rDNA trees contain three long branches: *Plasmodium* spp., the crustacean gregarines (Cephaloidophoroidea), and *Gregarina niphandrodes*. Exclusion of non-alveolate outgroups and each long branch from the alignment, as it was recommended by Bergsten (2005), for detection of long branch attraction artifact (LBA) influence (the tree topology should change if it is present), did not significantly change the tree topology in our ML analyses (data not shown). Bergsten (2005) also concluded that increasing of alignment length does not improve upon, but instead, strengthens LBA effect. However, our analyses of concatenated rDNAs showed an improvement in the "best tree" topology (it was getting closer to that which would be expected, based on previous work), and support for nodes also increased (Table 3). Therefore, it is likely that one of the main reasons for "bad" topologies are datasets that are limited, with low phylogenetic signal, rather than LBA alone.

Including a greater number of characters in phylogenetic analyses can partially compensate for limited taxon sampling, despite the presence of long branches. It is also likely that improving in tree topology and support was the result of the gregarine LSU rDNA having a lower relative rate of evolution (Table 4, Fig. 7). Branch lengths among gregarine apicomplexans tended to remain the same length, while branch lengths in other apicomplexan lineages tended increase 1.5 to 2 times in length. Since variability in DNA and evolutionary rates should correspond to branch length, we can suppose that the regions of the LSU rDNA used in the phylogenetic analyses are more variable (on average about 1.5 times) than those of SSU rDNA in the majority of apicomplexans. However, the *relative* variability (or relative evolutionary rate) of the aligned regions of gregarine LSU rDNA is lower than that of SSU rDNA, and this resulted in a more balanced pattern of branch lengths in our LSU trees. Similar situations seem to exist among other fast-evolving apicomplexan lineages such as *Plasmodium* spp., as well as other gregarine lineages. We think that this is the main reason for a considerably better result in our phylogenetic analyses using LSU rDNA, in comparison with those datasets containing only SSU rDNA. Thus, our analyses containing relatively few, highly-diverged sequences have demonstrated the promising application of LSU rDNA for phylogenetic inferences among apicomplexans.

The exploration of LSU rDNA as a phylogenetic marker for apicomplexans will require further studies and broader taxon sampling. The problem lies in the limited number of LSU rDNA sequences available to date. Protein-coding genes might also contribute to the resolution of the apicomplexans backbone. However, available protein-coding sequences for gregarines are also limited and, additionally, subject to high evolutionary rates (Leander *et al*. 2003a).

**Remarks on gregarine morphology**

The monophylic grouping of gregarines from crustaceans (Cephaloidophoroidea) prompts us to identify common morphologica traits between trophozoite and gamonts. With regard to gregarine morphology, it is necessary to distinguish between trophozoites (attached feeding stages according to Levine's terminology (Levine 1971) and mature gamonts. The latter are free stages dedicated to the formation of syzygy, which have been detached from the host cell in a natural way. We consider all the solitary gregarine individuals studied here as gamonts because we dealt with free individuals, which were obviously full-grown, looked similar to syzygy partners, and demonstrated no obvious damages or drops of cytoplasm on their forebodies.

Previous studies on *Cephaloidophora communis* were conducted under magnifications too low for re-

vealing the fine cell structure of this gregarine (histological study by Lacombe *et al*. 2002). Our investigation has demonstrated that structure of the cells, as viewed under light and electron microscopy, correspond to each other. For instance, there are two septa in the gamonts of *C.* cf. *communis*, namely the protomerite/deutomerite septum, which has been documented in a diverse set of families including the Actinocephalidae, Didymophyidae, Gregarinidae, Leidyanidae, and Stylocephalidae (Devauchelle 1968a, Desportes 1969, Baudoin and Ormières 1973, Ormières and Daumal 1970a, b, Hildebrand 1976, Ormières 1977, Tronchin and Schrével 1977, Valigurová and Koudela 2005, Valigurová *et al*. 2007, Valigurová 2012), and the distinct septum between the epimerite and the protomerite, observed in gregarines for the first time here. The small lenticular epimerite (cephaloid) is characteristic of this genus, which is reflected in the generic diagnosis of *Cephaloidophora* (Clopton 2000). This epimerite differs from the previously studied gregarine species (see above) in that it is not discarded after trophozoite detachment. It contains no large vacuoles, mitochondria, or fibril bundles, and it is filled with electron dense vesicles. These vesicles, resembling micronemes, seem to release some glutinous secretion through the pores. Previously, numerous pores have been described in *C.* cf. *communis* epimerite using SEM (Rueckert *et al*. 2011b). We observed the attachment (gluing) of living gregarines to a glass slide by the anterior end after a long-term incubation in seawater. We suppose this is likely the natural and only way of attachment for this gregarine. The previous light microscopic study of *C. communis* in the host intestine revealed no protruded epimerite (Lacombe *et al*. 2002). The possible reason is that trophozoites undergo intracellular development (Poisson 1924), which evidently does not require a complicated attachment apparatus. In this context, we propose to use the term "cephaloid" for the anterior end of *C.* cf. *communis* to emphasize its distinct difference from those of other gregarines with the discardable or condensable epimerite.

Concerning *Heliospora* cf. *longissima,* the situation is more difficult, because the primite and the satellite of the syzygy are organized differently and, in addition, the structure of the primite using electron microscopes (presence of just one septum) doesn't correspond to those found in light micrographs (two septa are visible). Using light microscopy, there is a distinct light-refracting border marking some structure(s) in the cytoplasm, be it a fibrillar phragma or (probably) something else. In *H.* cf. *longissima,* this apparent epi-/protomerite septum could be a layer of electron-dense granules (Fig. 4C). The same granules probably reinforce a border, which is seen in light micrographs as the proto-/deutomerite septum, since the real septum seems too loose and is difficult to discern in some micrographs. Unfortunately, comparison with the data on other *Heliospora* species, which could solve this discrepancy, is impossible since these gregarines have not been studied by TEM. Regarding direct comparison with TEM data from other putatively related gregarines (e.g. *Uradiophora*), there are some doubts in this kinship, as explained below.

The genus *Heliospora* was included in Uradiophoridae family by Grassé (1953), based on parasitism in crustaceans and its cylindrical epimerite. The drawing of *H. longissima* presented by Grassé (1953) was obviously done from individuals fixed in syzygy, which had undergone deformation (a usual situation with fixed gregarines). However, the living gregarines have rather dome-shaped or lenticular epimerite, which is rather similar to the cephaloid of *Cephaloidophora*. Judging on existing images (see Fig. 3.90 in: Desportes and Schrével 2013), the forebody morphology of representatives of the type genus *Uradiophora* strongly differs from *Heliospora*. Their forebody is elongated and bears an anterior crown of hair- or finger-like processes (the attachment apparatus), and contains a bulky axial fibrillar structure, surrounded by large vacuoles. This is visible both at the light microscopic and ultrastructural levels (in *U. maetzi*, see Desportes and Théodoridès 1985), and has never been reported for any *Heliospora* spp. This attachment apparatus has contradictory interpretations that have described this as a protomerite (Desportes and Théodoridès 1985, Desportes and Schrével 2013, page 85), or even as a mucron (Desportes and Schrével, 2013, page 346). According to the TEM data, a proto-/deutomerite septum in *U. maetzi* is absent in this specific developmental stage, but it is clearly visible on the light microscopy drawings of several *Uradiophora* spp. (Desportes and Théodoridès 1985, Desportes and Schrével 2013, Fig. 3.90). Additionally, there is a difference in the epicyte structure between *U. maetzi* and *H.* cf. *longissima*. Epicytic folds of the former species contain axial electron-dense matter in the tops of the folds (like in *Ganymedes*, *Porospora*, *Thiriotia*) whereas epicytic folds of the latter species obviously lack this (e.g., *Cephaloidophora*) (Desportes and Théodoridès 1985, Desportes and Schrével 2013, Desportes *et al*. 1977, this study). Thus, the close relations between *Heliospora* and *Uradiophora* are intrigu-

ing and questionable, especially in view of the absence of molecular phylogenetic data.

Regarding terminology used in diagnoses of gregarine taxa (e.g., diagnoses of the genus *Cephaloidophora* in the reviews Clopton 2000, Desportes and Schrével 2013), three weak points should be noted: (i) it is not always clear what characteristic belongs to which lifecycle stage (e.g., trophozoite or gamont), (ii) the terms "trophozoites" and "gamonts" are used interchangeably, and (iii) discrepancies in light and electron micrographs can exist (appearance of a septum, which can be actually absent).

It seems logical to modify the terminology for the trophozoite and gamont morphology to reflect both the number of sections within the body and the number of septa, in order to make some of these issues less ambiguous. A possible option might be to use the terms "mono-", "di-", and "tricystid" gregarine morphology based on light micrographs. The terms "aseptate" and "septate", that indicate the number of the septa, might be exclusively used for descriptions and diagnoses based on transmission electron micrographs. For instance, gamonts of *Lecudina* spp. are monocystid (border is absent) and aseptate; *Gregarina* spp. are dicystid, uniseptate; *Cephaloidophora* cf. *communis* is tricystid and biseptate; *Helispora* cf. *longissima* is tricystid uniseptate. Future studies and species descriptions or re-descriptions are advisable, in order to provide data using transmission electron microscopy. This could improve gregarine taxonomy and our understanding of some aspects of gregarine physiology, especially the role of the septum in gregarine feeding.

In past studies, molecular phylogenetic data demonstrated that the robust clade of gregarines parasitizing crustaceans (Cephaloidophoroidea) contains four subclades (Rueckert *et al*. 2011b). Two of them, corresponding to the families Cephaloidophoridae and (possibly) Uradiophoridae (see above about *Heliospora* taxonomy), include septate forms. The third clade corresponds to the family Porosporidae. The protomerite/ deutomerite septum in this clade is implicit or even missing (e.g., in *Thiriotia pugettiae*). All these families belong to the suborder Septata (Clopton 2000). Note, the genus *Thiriotia* has been removed in a recently established family, Thiriotiidae (Desportes and Schrével 2013). The last, most basal subclade, corresponds to the family Ganymedidae of the suborder Aseptata, which has no septa ("monocystid" or "aseptate" forms). Thus, the presence of a septum is not a trait shared by all these gregarines. This leads us to propose that the septum (septa) could have either (i) emerged in advanced Cephaloidophoroidea forms (Cephaloidophoridae and, putatively, Uradiophoridae), independent of other septate gregarines (homoplasy), or (ii) the presence of a septum is the ancestral state for this clade, but it was secondarily lost in Ganymedidae. Unfortunately, the physiological role of the septum remains unclear, which does not allow us to specifically consider the factors underlying its emergence or the advantages it provides to the parasite cell.

All gregarines from crustaceans studied by transmission electron microscopy (*Porospora portunidarum, Thiriotia pisae, Ganymedes vibiliae, G. eucopiae*, *Uradiophora maetzi, Cephaloidophora* cf. *communis*, and *Heliospora* cf. *longissima*) have a similar structure of epicytic folds (Desportes *et al*. 1977, Desportes and Théodoridès 1985, Desportes and Schrével 2013, this study). On cross-sections they are narrow with bulged tops, containing a few (3–6) rippled, dense structures and 2–5 apical filaments, with exeption of *Ganymedes* having 9 filaments. Additionally, many of them have electron-dense axial matter in the tops of the epicytic folds, however, it is clearly absent in *C.* cf. *communis* and *H.* cf. *longissima.* On the other hand, these characteristics are present also in other, unrelated gregarines. Swollen tops are observed in *Gregarina polymorpha*, and *Gregarina steini* has epicytic folds almost identical with *C.* cf. *communis* (3 apical arcs, and 2 apical filaments). These also contain the electron dense axial matter within the tops of the folds (Valigurová *et al*. 2013). The aseptate gregarine *Gonospora beloneides* (Urosporidae) has folds with swollen tops, containing the electron-dense axial matter as well, but also contains 9 apical arcs and filaments (Corbel *et al*. 1979). Thus, we conclude that our data on the epicyte structure highlights the morphological diversity of gregarines belonging to Cephaloidophoroidea. However, these ultrastructural characters do not present any distinct synapomorphies of the group. Consequently, this group shares only the two following characters:

- Parasitism in the intestines of crustacean hosts.
- Close relationship based on molecular data (rDNA).

These results, while contradicting some aspects of the Levine's taxonomical scheme of Eugregarinida, which divides this group based on the presence or absence of a septum (Levine 1985, Clopton 2000), do support views by Grassé (1953), who placed the families of gregarines from crustaceans together, rather than spread among various suborders. However, a justified decision between the systems requires further molecu-

lar phylogenetic studies, spanning the taxonomic diversity of gregarines. In particular, LSU rDNA sequencing may contribute to the phylogeny of these lower apicomplexans.

**Aknowledgements.** This study used the Bioportal at University of Oslo (www.bioportal.uio.no) and the Chebyshov Supercomputer Center of Lomonosov Moscow State University (http://parallel.ru/cluster) to make phylogenetic computations. DNA sequencing was performed at the DNA sequencing center "Genome" (Engelhardt Institute of Molecular Biology, Russian Academy of Sciences, www.genome-centre.ru). The electron microscopic studies were performed at User Facilities Center of Lomonosov Moscow State University under financial support of Ministry of Education and Science of Russian Federation.

The work was supported by grant NSH–1801.2014.4 from the Council of the President of the Russian Federation and grants from the Russian Foundation of Basic Researches (09-04-01682, 11-04-90778, and 15-29-02601), Ministry of Education and Science of Russian Federation (Federal Target Program "Scientific and scientific-pedagogical personnel of innovative Russia 2009–2013"), and ECIP – Centre of excellence GAČR No.GBP505/12/G112 (Czech Republic). The funders had no role in study design, data collection, analyses, decision to publish, or preparation of the manuscript. Our thanks are due to Dr. Dmitry Scherbakov (Limnological Institute, Siberian branch of the Russian Academy of Sciences, Irkutsk) for his help in organizing the expedition to Lake Baikal, to Dr. Nikita Vassetzky (Engelhardt Institute of Molecular Biology, Russian Academy of Sciences) for translating this article into English, and to Dr. Kevin Wakeman (University of British Columbia, Canada) for reading the manuscript.

## REFERENCES

Adl S. M., Simpson A. G. B., Lane C. E., Lukeš J., Bass D., Bowser S. S., Brown M. W., Burki F., Dunthorn M., Hampl V., Heiss A., Hoppenrath M., Lara E., le Gall L., Lynn D. H., McManus H., Mitchell E. A. D., Mozley-Stanridge S. E., Parfrey L. W., Pawlowski J., Rueckert S., Shadwick L., Schoch C. L., Smirnov A., Spiegel F. W. (2012) The revised classification of eukaryotes. *J. Eukaryot. Microbiol*. **59:** 429–493

Alfaro M. E., Zoller S., Lutzoni F. (2003) Bayes or bootstrap? A simulation study comparing the performance of Bayesian Markov Chain Monte Carlo sampling and bootstrapping in assessing phylogenetic confidence. *Mol. Biol. Evol*. **20:** 255–266

Bergsten J. (2005) A review of long-branch attraction. *Cladistics* **21:** 163–193

Baudoin J., Ormières R. (1973) Sur quelques particularités de l'ultrastructure de *Didymophyes chaudefouri* Ormières, Eugregarine, Didymophyidae. *C. R. Acad. Sci*. D. **277:** 73–75

Bourlat S. J., Nielsen C., Economou A. D., Telford M. J. (2008) Testing the new animal phylogeny: A phylum level molecular analysis of the animal kingdom. *Mol. Phylogenet. Evol.* **49:** 23–31

Campbell V., Lapointe F.-J. (2009) The use and validity of composite taxa in phylogenetic analysis. *Syst. Biol*. **58:** 560–572

Cleary A. C., Durbin E. G., Rynearson T. A. (2012) Krill feeding on sediment in the Gulf of Maine (North Atlantic). *Mar. Ecol. Prog. Ser*. **455:** 157–172

Clopton R. E. (2000) Order Eugregarinorida Leger, 1900. In: An Illustrated Guide to the Protozoa (Eds. J. J. Lee, G. F. Leedale, P. Bradbury). Society of Protozoologists, Lawrence, KS, 205–288

Clopton R. E. (2009) Phylogenetic relationships, evolution, and systematic revision of the septate gregarines (Apicomplexa: Eugregarinorida: Septatorina). *Comp. Parasitol*. **76:** 167–190

Corbel J.-C., Desportes I, Théodoridès J. (1979). Étude de *Gonospora beloneides* (Ming.) (=*Lobianchella beloneides* Ming.) (grégarine Urosporidae), parasite coelomique d' une Alciopidae (Polychaeta) et remarques sur d'autres grégarines d' Alciopidae. *Protistologica* **15:** 55–65

Cummings M. P., Handley S. A., Myers D. S., Reed D. L., Rokas A., Winka K. (2003) Comparing bootstrap and posterior probability values in the four-taxon case. *Syst. Biol*. **52:** 477–487

Dallai R., Vegni Talluri M. (1988) Evidence for septate junctions in the syzygy of the protozoon *Gregarina polymorpha* (Protozoa, Apicomplexa). *J. Cell Sci*. **89:** 217–224

Delsuc F., Brinkmann H., Chourrout D., Philippe H. (2006) Tunicates and not cephalochordates are the closest living relatives of vertebrates. *Nature* **439:** 965–968

Desportes I. (1969) Ultrastructure et développement des Grégarines du genre *Stylocephalus*. *Ann. Sci. Nat. Zool*. Ser. 12. **11:** 31–96

Desportes I. (1974) Ultrastructure et evolution nucléaire des trophozoïtes d'une Grégarine d'Ephéméroptère: *Enterocystis fungoides* M. Codreanu. *J. Protozool*. **21:** 83–94

Desportes I., Théodoridès J. (1985) Particularités cytologiques d' *Uradiophora maetzi* Théod. et Desp. (Eugregarina, Uradiophoridae) parasite du Mysidace bathypelagique *Gnathophausia zoea* WS. *Ann. Sci. Nat. Zool. Ser*. 13. **7:** 199–213

Desportes I., Schrével J. (Eds.) (2013) Treatise on Zoology – Anatomy, Taxonomy, Biology. The Gregarines. Brill, Leiden, 2 vols

Desportes I., Vivarès C. P., Théodoridès J. (1977) Intérêt taxinomique de l'ultrastructure épicytaire chez *Ganymedes* Huxley, *Porospora* Schneider et *Thiriotia* n.g. Eurégarines parasites de Crustacés. *Ann. Sci. Nat. Zool. Ser*. 12. **19:** 261–277

Devauchelle G. (1968a) Étude ultrastructurale du développement des Grégarines du *Tenebrio molitor* L. *Protistologica* **4:** 313–332

Devauchelle G. (1968b) Étude ultrastructurale de *Gregarina polymorpha* (Hamm.) en syzygie. *J. Protozool.* **15:** 629–636

Douady C. J., Delsuc F., Boucher Y., Doolittle W. F., Douzery E. J. P. (2003) Comparison of Bayesian and maximum likelihood bootstrap measures of phylogenetic reliability. *Mol. Biol. Evol.* **20:** 248–254

Dyakin A. Y., Simdyanov T. G. (2005) The cortical zone of skittle-like cells of *Urospora chiridotae*, a gregarine from an apode holothuria *Chiridota laevis*. *Protistology* **4:** 97–105

Edgar R. C. (2004) MUSCLE: multiple sequence alignment with high accuracy and high throughput. *Nucleic Acids Res*. **35:** 1792–1797

Edgcomb V.P., Beaudoin D., Gast R., Biddle J.F., Teske A. (2011) Marine subsurface eukaryotes: the fungal majority. *Environ. Microbiol*. **13:** 172–183

Erixon P., Svennblad B., Britton T., Oxelman B. (2003) Reliability of Bayesian posterior probabilities and bootstrap frequencies in phylogenetics. *Syst. Biol*. **52:** 665–673

Felsenstein J. (1985) Confidence limits on phylogenies: an approach using the bootstrap. *Evolution* **39:** 783–791

Floyd R. M., Abebe E., Papert A., Blaxter M. L. (2002) Molecular barcodes for soil nematode identification. *Mol. Ecol*. **11:** 839–850

Frolov A. O. (1991) World fauna of gregarines. Family Monocystidae. Zool. Inst. Acad. Sci. USSR, Leningrad (in Russian with English summary)

Grassé P.-P., Théodoridès J. (1959) Recherches sur l'ultrastructure de quelques Grégarines. *Ann. Sci. Nat. Zool.* Ser. 12. **1:** 296–305

Grassé P.-P. (1953) Classe des Grégarinomorphes. In: Traité de Zoologie (Ed. P.-P. Grassé). Masson, Paris, 550–690

Hall T. A. (1999) BioEdit: a user–friendly biological sequence alignment editor and analysis program for Windows 95/98/NT. *Nucl. Acid. Sym*. Ser. **41:** 95–98

Hildebrand H. F. (1976) Elektronenmikroskopische Untersuchungen an den Entwicklungstadien des Trophozoiten von *Didymophyes gigantea* (Sporozoa, Gregarinida). 1. Die Feinstruktur des Proto- und Epimeriten und die Beziehung zwischen Wirt und Parasit. *Z. Parasitenk.* **49:** 193–215

Hildebrand H. F. (1981) Elektronenmikroskopische Untersuchungen an den Entwicklungsstadien des Trophozoiten von *Didymophyes gigantea* (Sporozoa, Gregarinida). 3. Die Feinstruktur des Epizyten mit besonderer Berücksichtigung der kontraktilen Elemente. *Z. Parasitenk*. **64:** 29–46

Hoshide K. (1975) Studies on the gregarines in Japan (Part 1). The fine structure of some gregarines. *Bull. Fac. Educ. Yamaguchi Univ.* **25:** 71–106

Janardanan K. P., Ramachandran P. (1983) Differential permeability of protomerite and deutomerite epicytes of the cephaline gregarine, *Stenoductus carlogoni* (Cephalina, Monoductidae) to cupric ions and vital stains. *Indian J. Exp. Biol*. **21:** 572–574

Jobb G. (2011) TREEFINDER version of March 2011. 2011. Munich, Germany. Distributed by the author at www.treefinder.de

Jobb G., von Haeseler A., Strimmer K. (2004) TREEFINDER: A powerful graphical analysis environment for molecular phylogenetics. *BMC Evol. Biol*. **4:** 18

Kishino H., Hasegawa M. (1989) Evaluation of the maximum likelihood estimate of the evolutionary tree topologies from DNA sequence data, and the branching order in hominoidea. *J. Mol. Evol*. **29:** 170–179

Lacombe D., Jakowska S., Silva E. (2002) Gregarine *Cephaloidophora communis* Mawrodiadi, 1908 in the barnacle *Euraphia rhyzophorae* Oliveira, 1940 from Brazil. *Mem. Inst. Oswaldo Cruz* **97:** 1057–1061

Landers S.C. (2002) The fine structure of the gamont of *Pterospora floridiensis* (Apicomplexa: Eugregarinida). *J. Eukaryot. Microbiol*. **49(3):** 220–226

Landers S.C. and Leander B. S. (2005) Comparative surface morphology of marine coelomic gregarines (Apicomplexa, Urosporidae): *Pterospora floridiensis* and *Pterospora schizosoma*. *J. Eukaryot. Microbiol*. **52:** 23–30

Leander B. S. (2007) Molecular phylogeny and ultrastructure of *Selenidium serpulae* (Apicomplexa, Archigregarinia) from the calcareous tubeworm *Serpula vermicularis* (Annelida, Polychaeta, Sabellida). *Zool. Scripta* **36:** 213–227

Leander B. S., Keeling P. J. (2004) Early evolutionary history of dinoflagellates and apicomplexans (Alveolata) as inferred from hsp90 and actin phylogenies. *J. Phycol*. **40:** 341–350

Leander B. S., Clopton R. E., Keeling P. G. (2003a) Phylogeny of gregarines (Apicomplexa) as inferred from SSU rDNA and β-tubulin. *Int. J. Syst. Evol. Microbiol.* **53:** 345–354

Leander B. S., Harper J. T., Keeling P. G. (2003b) Molecular phylogeny and surface morphology of marine aseptate gregarines (Apicomplexa): *Selenidium* spp. and *Lecudina* spp. *J. Parasitol*. **89:** 1191–1205

Leander B. S., Lloyd S. A. J., Marshall W., Landers S. C. (2006) Phylogeny of marine gregarines (Apicomplexa) – *Pterospora*, *Lithocystis* and *Lankesteria* – and the origin(s) of coelomic parasitism. *Protist* **157:** 45–60

Levine N. D. (1970) Taxonomy of the Sporozoa. *J. Parasitol*. **56 (sec. 2):** 208–209

Levine N. D. (1971) Uniform terminology for the protozoan subphylum Apicomplexa. *J. Protozool.* **18:** 352–355

Levine N. D. (1979) New genera and higher taxa of septate gregarines (Protozoa, Apicomplexa). *J. Protozool*. **26:** 532–536

Levine N. D. (1984) Nomenclatural corrections and new taxa in the apicomplexan Protozoa. *Trans. Am. Microsc. Soc*. **103:** 195–204

Levine N. D. (1985) Phylum 2. Apicomplexa Levine, 1970. In: An Illustrated Guide To The Protozoa (Eds. J. J. Lee, S. H. Hutner, E. C. Bovee). Society of Protozoologists, KS, 322–374

Levine N. D. (1988a) The protozoan phylum Apicomlexa. CRC Press, Boca Raton, FL, 2 vols

Levine N. D. (1988b) Progress in taxonomy of the apicomplexan Protozoa. *J. Protozool*. **35:** 518–520

Levine N. D., Corliss J. O., Cox F. E. G., Deroux G., Grain J., Honigberg B. M., Leedale G. F., Loeblich A. R., Lom J., Lynn D., Merinfeld E. G., Page F. C., Poljansky G., Sprague V., Vavra J., Wallace F. G. (1980) A newly revised classification of the Protozoa. *J. Protozool.* **27:** 37–58

MacMillan W. G. (1973a) Conformation changes in the cortical region during peristaltic movements of a gregarine trophozoite. *J. Protozool*. **20:** 267–274

Marques A., Ormières R., Puissegur C. (1978) Observations en microscopie électronique a balayage de quelques stades de *Trichorhynchus pulcher* Schneider, 1882, Eugrégarine parasite de *Scutigera* (Myriapodes, Chilopodes). *Ann. Sci. Nat. Zool*. **20:** 27–36

Mercier C., Schrével J., Stark J.R. (1973) The storage polysaccharide (paraglycogen) of the gregarine, *Gregarina blaberae*: cytology and biochemistry. *Comp. Biochem. Physiol*. **44B:** 1001–1010

Miles H. B. (1968) The fine structure of the epicyte of the acephaline gregarines *Monocystis lumbrici–olidi,* and *Nematocystis magna*: observations by electron microscope. *Rev. Iber. Parasitol.* **28:** 455–465

Ormières R. (1977) *Pyxinia firmus* (Léger 1892), Eugrégarine parasite du Coléopter *Dermestes frischi* Kugel. Étude ultrastructurale. *Z. Parasitenk*. **53:** 13–22

Ormières R., Daumal J. (1970a) Données ultrastructurales sur *Epicavus araeoceri* Orm. Daum., eugrégarine parasite d`*Araeocerus fasciculatus* de Geer (Coléoptere; Anthribidae). *C. R. Acad. Sci.* D. **270:** 2451–2453

Ormières R., Daumal J. (1970b) Étude ultrastructurale de la partie antérieure d'*Epicavus araeoceri* Ormières, Daumal, eugregarine parasite du coléoptere Anthribidae *Araeocerus fascilulatus* de Geer. *Protistologica* **6:** 97–111

Perkins F. O., Barta J. R., Clopton R. E., Peirce M. A., Upton S. J. (2000) Phylum Apicomplexa. In: An Illustrated Guide to the Protozoa (Eds. J. J. Lee, G. F. Leedale, P. Bradbury). Society of Protozoologists, Lawrence, KS, 190–370

Petrov N. B., Pegova A. N., Manylov O. G., Vladychenskaya N. S., Mugue N. S., Aleshin V. V., (2007) Molecular phylogeny of Gastrotricha on the basis of a comparison of the 18S rRNA genes: rejection of the hypothesis of a relationship between Gastrotricha and nematoda. *Mol. Biol*. **41:** 445–452

Philippe M. (1983) Differentiation and cellular arrangement of *Gregarina blaberae* gamonts. *J. Protozool.* **30:** A72

Philippe H., Snell E. A., Bapteste E., Lopez P., Holland P. W. H., Casane D. (2004) Phylogenomics of Eukaryotes: Impact of Missing Data on Large Alignments. *Mol. Biol. Evol.* **21:** 1740–1752

Poisson R. (1924) Sur quelques Grégarines parasites de Crustacés, observées à Luc–sur–mer (Calvados). *Bull. Soc. Zool. France* **49:** 238–248

Porchet-Henneré E., Fischer A. (1973) *Diplauxis schreveli,* n. sp., Grégarine parasite du coelome de l'Annélide Polychète *Platynereis dumerilli*: cycle et étude ultrastructurale préliminaire. *Protistologica* **9:** 437–454

Ronquist F., Huelsenbeck J. P. (2003) MrBayes 3: Bayesian phylogenetic inference under mixed models. *Bioinformatics* **19:** 1572–1574

Rueckert S., Leander B. S. (2008) Morphology and phylogenetic position of two novel marine gregarines (Apicomplexa, Eugregarinorida) from the intestines of North-Eastern Pacific ascidians. *Zool. Scripta* **37:** 637–645

Reynolds E.S. (1963) The use of lead citrate at high pH as an electron opaque stain in electron microscopy. *J. Cell Biol*. **17:** 208–212

Rueckert S., Leander B. S. (2009) Molecular phylogeny and surface morphology of marine archigregarines (Apicomplexa), *Selenidium* spp., *Filipodium phascolosomae* n. sp. and *Platyproteum* n. g. and comb. from North-Eastern Pacific peanut worms (Sipuncula). *J. Eukaryot. Microbiol.* **56:** 428–439

Rueckert S., Leander B. S. (2010) Description of *Trichotokara nothriae* n. gen. et sp. (Apicomplexa, Lecudinidae) – an intestinal gregarine of *Nothria conchylega* (Polychaeta, Onuphidae). *J. Invertebr. Pathol*. **104:** 172–179

Rueckert S., Chantangsi C., Leander B. S. (2010) Molecular systematics of marine gregarines (Apicomplexa) from North-Eastern Pacific polychaetes and nemerteans, with descriptions of three novel species: *Lecudina phyllochaetopteri* sp. nov., *Difficilina tubulani* sp. nov. and *Difficilina paranemertis* sp. nov. *Int. J. Syst. Evol. Microbiol*. **60:** 2681–2690

Rueckert S., Villette P. M. A. H., Leander B. S. (2011a) Species boundaries in gregarine apicomplexan parasites: a case study – comparison of morphometric and molecular variability in *Lecudina* cf. *tuzetae* (Eugregarinorida, Lecudinidae). *J. Eukaryot. Microbiol.* **58:** 275–283

Rueckert S., Simdyanov T. G., Aleoshin V. V., Leander B. S. (2011b) Identification of a divergent environmental DNA sequence clade using the phylogeny of gregarine parasites (Apicomplexa) from crustacean hosts. *PLoS ONE* **6:** e18163. doi:10.1371/journal.pone.0018163

Rueckert S., Wakeman K. C., Leander B. S. (2013) Discovery of a diverse clade of gregarine Apicomplexans (Apicomplexa: Eugregarinorida) from Pacific eunicid and onuphid polychaetes, including descriptions of *Paralecudina* n. gen., *Trichotokara* japonica n. sp., and *T. eunicae* n. sp. *J. Eukaryot. Microbiol*. **60:** 121–136

Schrével J., Caigneaux E., Gros D., Philippe M. (1983) The three cortical membranes of the gregarines. I. Ultrastructural organization of *Gregarina blaberae*. *J. Cell Sci*. **61:** 151–174

Shimodaira H. (2002) An approximately unbiased test of phylogenetic tree selection. *Syst. Biol*. **51:** 492–508

Shimodaira H., Hasegawa M. (1999) Multiple comparisons of log-likelihoods with applications to phylogenetic inference. *Mol. Biol. Evol*. **16:** 1114–1116

Simdyanov T. G. (1995) Two new species of gregarines with the aberrant structure of epicyte from the White Sea. *Parazitologiya* **29**: 305–315

Simdyanov T. G. (2004) *Sphinctocystis phyllodoces* gen. n., sp. n. (Eugregarinida: Lecudinidae) – a new gregarine from *Phyllodoce citrina* (Polychaeta: Phyllodocidae). *Parazitologiya* **38:** 322–332

Simdyanov T. G. (2009) *Difficilina cerebratuli* Gen. et sp. n. (Eugregarinida: Lecudinidae) – a new gregarine species from the nemertean *Cerebratulus barentsi* (Nemertini: Cerebratulidae). *Parazitologiya* **43:** 273–287

Stamatakis A. (2006) RAxML-VI-HPC: maximum likelihood-based phylogenetic analyses with thousands of taxa and mixed models. *Bioinformatics* **22:** 2688–2690

Strimmer K., Rambaut A. (2002) Inferring confidence sets of possibly misspecified gene trees. *Proc. Roy. Soc*. B. **269:** 137–142

Templeton T. J., Enomoto S., Chen W. J., Huang C. G., Lancto C. A., Abrahamsen M. S., Zhu G. (2010) A genome-sequence survey for *Ascogregarina taiwanensis* supports evolutionary affiliation but metabolic diversity between a gregarine and *Cryptosporidium*. *Mol. Biol. Evol*. **27:** 235–248

Toso M. A., Omoto C. K. (2007) *Gregarina niphandrodes* may lack both a plastid genome and organelle. *J. Eukaryot. Microbiol*. **54:** 66–72

Tronchin G., Schrével J. (1977) Chronologie des modifications ultrastructurales au cours de la croissance de la *Gregarima blaberae*. *J. Protozool*. **24:** 67–82

Valigurová A. (2012) Sophisticated adaptations of *Gregarina cuneata* (Apicomplexa) feeding stages for epicellular parasitism. *PLoS ONE* **7:** e42606

Valigurová A., Hofmannová L., Koudela B., Vávra J. (2007) An ultrastructural comparison of the attachment sites between *Gregarina steini* and *Cryptosporidium muris*. *J. Eukaryot. Microbiol.* **54:** 495–510

Valigurová A., Koudela B. (2005) Fine structure of trophozoites of the gregarine *Leidyana ephestiae* (Apicomplexa: Eugregarinida) parasitic in *Ephestia kuehniella* larvae (Lepidoptera). *Eur. J. Protistol*. **41:** 209–218

Valigurová A., Michalková V., Koudela B. (2009) Eugregarine trophozoite detachment from the host epithelium via epimerite retraction: fiction or fact? *Int. J. Parasitol.* **39:** 1235–1242

Valigurová A., Vaskovicová N., Musilová N. Schrével J. (2013) The enigma of eugregarine epicytic folds: where gliding motility originates? *Frontiers in Zoology* **10:** 57

Van der Auwera G., Chapelle S., De Wachter R. (1994) Structure of the large ribosomal subunit RNA of *Phytophtora megasperma*, and phylogeny of the oomycetes. *FEBS Letters* **338:** 133–136

Vinckier D. (1969) Organisation ultrastructurale corticale de quelques Monocystidees parasites du ver Oligochete *Lumbricus terrestris* L. *Protistologica* **5:** 505–517

Vinckier D., Vivier E. (1968) Organisation ultrastructurale corticale de la gregarine *Monocystis herculea*. *C. R. Acad. Sci*. D. **266:** 1737–1739

Vivier E. (1968) L'organisation ultrastructurale corticale de la Grégarine *Lecudina pellucida*; ses rapports avec l'alimentation et la locomotion. *J. Protozool*. **5:** 230–246

Vivier E., Devauchelle G., Petitprez A., Porchet-Henneré E., Prensier G., Schrével J., Vinckier D. (1970) Observations de cytologie comparée chez les Sporozoaires. I. – Les structures superficielles chez les formes végétatives. *Protistologica* **6:** 127–150

Wakeman K. C., Leander B. S. (2012) Molecular phylogeny of pacific archigregarines (Apicomplexa), including descriptions of *Veloxidium leptosynaptae* n. gen., n. sp., from the sea cucumber *Leptosynapta clarki* (Echinodermata), and two new species of *Selenidium*. *J. Eukaryot. Microbiol*. **59:** 232–245

Wakeman K. C., Leander B. S. (2013) Identity of environmental DNA sequences using descriptions of four novel marine gregarine parasites, *Polyplicarium* n. gen. (Apicomplexa), from capitellid polychaetes. *Mar. Biodivers*. **43:** 133–147

Walker M. H., Lane N. J. (1982) Freeze-fracture studies on the epicyte of *Gregarina garnhami*. *J. Protozool*. **29:** 640

Received on 9th May, 2014; revised on 16th November, 2014; accepted on 21st November, 2014